SAN FRANCISCO ESTUARY & WATERSHED SCIENCE
Sponsored by the Delta Science Program and the UC Davis Muir Institute

RESEARCH

Use of a Managed Flow Pulse as Food Web Support for Estuarine Habitat

Jared Frantzich*[1], Brittany E. Davis[1], Michael MacWilliams[2], Aaron Bever[2], Ted Sommer[1]

ABSTRACT

While freshwater inflow has been a major focus of resource management in estuaries, including the upper San Francisco Estuary, there is a growing interest in using focused flow actions to maximize benefits for specific regions, habitats, and species. As a test of this concept, in summer 2016, we used a managed flow pulse to target an ecologically important region: a freshwater tidal slough complex (Cache Slough Complex–CSC). Our goal was to improve estuarine habitat by increasing net flows through CSC to enhance downstream transport of lower trophic-level resources, an important driver for fishes such as the endangered Delta Smelt *Hypomesus transpacificus*. We used regional water infrastructure to direct 18.5 million m^3 of Sacramento River flow into its adjacent Yolo Bypass floodplain, where the pulse continued through CSC. Simulations using a 3-D hydrodynamic model (UnTRIM) indicated that the managed flow pulse had a large effect on the net flow of water through Yolo Bypass, and between CSC and further downstream. Multiple water quality constituents (specific conductivity, dissolved oxygen, nutrients [NO_3 + NO_2, NH_4, PO_4]) varied across the study region, and showed a strong response to the flow pulse. In addition, the lower Sacramento River had increased phytoplankton biomass and improved food quality indices (estimated from long-chain essential fatty acids) after the flow pulse. The managed flow pulse resulted in increased densities of zooplankton (copepods, cladocerans) demonstrating potential advection from upper floodplain channels into the target CSC and Sacramento River regions. This study was conducted during a single year, which may have had unique characteristics; however, we believe that our study is an instructive example of how a relatively modest change in net flows can generate measurable changes in ecologically relevant metrics, and how an adaptive management action can help inform resource management.

KEY WORDS

Yolo Bypass, flow pulse, food subsidy, plankton, water quality, management action

SFEWS Volume 19 | Issue 3 | Article 3

https://doi.org/10.15447/sfews.2021v19iss3art3

* Corresponding author: Jared.Frantzich@water.ca.gov

1 California Department of Water Resources
West Sacramento, CA 95691 USA

2 Anchor QEA, LLC
San Francisco, CA 94111 USA

INTRODUCTION

The San Francisco Estuary, like many coastal regions, is a heavily impacted ecosystem, with major effects from urbanization, habitat degradation, water diversions, pollution, and invasive species (Lotze 2006, 2010; Worm et al. 2006). Given the extreme level of degradation of many of these areas, management strategies that improve both the structure and function of ecosystems are urgently needed. For improving ecosystem management in coastal aquatic regions, a variety of approaches have been used, including habitat restoration, flow augmentation, and contaminant and nutrient reduction (Zedler 2016). Such actions are most effective when organized in an adaptive management approach, where scientific information is used to guide design, evaluate project efficacy, and provide guidance for follow-up modifications or future projects (Delta Independent Science Board 2016 and Delta Science Program 2013). However, restoration and rehabilitation projects in coastal areas are often conducted without formal study designs or feedback loops to correct observed problems (Hennessey 2008; Thom 2000).

We conducted a large-scale flow experiment with a goal to improve transport and plankton food web conditions in a specific region of the upper San Francisco Estuary. Our hope was that the study results would provide insight for future management options for endangered fish habitat. Like other urbanized estuaries, the system suffers from multiple stressors related to anthropogenic effects, including diking and draining of wetlands, water diversions, channelization, invasive species, and contaminant inputs (Cloern and Jassby 2012; Nichols et al. 1986). These stressors have led to broad ecosystem changes, including a collapse of the fish communities in the upper estuary, leading to the listing of several species under the Endangered Species Act (Sommer et al. 2007; Thomson et al. 2010). Of these fishes, the most endangered is the Delta Smelt *Hypomesus transpacificus*, a small pelagic osmerid endemic to the upper San Francisco Estuary. The decline of this annual species is a resource management issue of national importance because the upper estuary is the primary water source for 8% of the US population and supplies a multi-billion-dollar agricultural industry (Moyle et al. 2018; Service 2007). Limitations on water diversions to protect Delta Smelt therefore have an important role in the water supply reliability of the region, which suffers from periodic drought.

One of the primary factors that has led to the federal and state listing of Delta Smelt as endangered is a decline in the planktonic food web (Rose et al. 2013; Sommer et al. 2007). Major declines have occurred in calanoid copepods, the primary dietary item for Delta Smelt, as well as in a suite of other zooplankton types (Winder and Jassby 2011). At the same time, there has been a major increase in smaller invasive species such as the copepod *Limnothoina* (Winder and Jassby 2011). The decline of native copepods is strongly related to the increased biomass of invasive bivalves (Kimmerer and Lougee 2015; Kimmerer and Orsi 1996), which filter much of the available phytoplankton and smaller life stages of native copepods. As a consequence, food limitation is a major driver that contributes to reduced survival, growth, and fecundity of Delta Smelt (Kimmerer and Rose 2018), and is thought to have resulted in low body condition and foraging success in studies of wild smelt (Bennett 2005; Hammock et al. 2015; Kimmerer and Rose 2018; Rose et al. 2013).

While food web resources have declined throughout much of the upper estuary, the Cache Slough Complex (CSC) in the north Delta region of the upper estuary (Figure 1) frequently has relatively higher levels of phytoplankton than other areas in the estuary (Downing et al. 2016; Lehman et al. 2010; Lehman et al. 2008). The region is notable because it retains some of the more complex tidal slough channels characteristic of the historical Delta, and is connected to the Yolo Bypass, a large floodplain (Sommer et al. 2001; Whipple et al. 2012) with higher plankton densities (Mahardja et al. 2019). The region therefore contains a much larger network of shallow habitat and long-residence-time channels, which are hypothesized to promote the development of planktonic food

resources (Lucas et al. 2009). As evidence of better habitat conditions in the CSC, the region is at least intermittently used by all life stages of Delta Smelt (Sommer and Mejia 2013). Based on these findings, CSC and the upstream Yolo Bypass have been targeted for major habitat restoration to improve food web conditions for Delta Smelt and other native species (Herbold et al. 2014; NMFS 2009).

Despite the potential benefits of the CSC to Delta Smelt and other species, the hydrology of the region is highly modified in drier seasons. Specifically, although the region is thought to be a major contributor to the downstream food web during the high-flow winter and spring (Sommer et al. 2004, Lehman et al. 2008), water diversions from the CSC and the upstream Yolo Bypass cause net negative (upstream) flows during drier months. Hence, there is a general upstream transport that directs food resources away from the habitats downstream of the CSC. A notable exception was during 2012, when unusually large agricultural flows through the Yolo Bypass and the CSC helped trigger the first fall phytoplankton bloom in the upper estuary in over 2 decades (Frantzich et al. 2018).

These observations led us to hypothesize that increased downstream net flow (e.g., at Lisbon Weir) during drier months would help to improve downstream transport of food web organisms in the CSC and perhaps stimulate downstream production of phytoplankton. To test these hypotheses, water was diverted via agricultural and flood infrastructure from the upstream Sacramento River into the tidal slough network of the lower Yolo Bypass and CSC. Our overall goal was to generate net downstream transport in the region, which we posited would improve habitat conditions. We predicted that this managed flow pulse (hereafter, flow pulse) would: (1) result in downstream transport of phytoplankton, zooplankton, and other chemical constituents from CSC to other areas of the San Francisco Estuary; and (2) help trigger further downstream primary production.

Note, however, that we do not specifically try to address the responses of Delta Smelt and the fish community to the hypothesized changes. The evaluation was already sufficiently complex with an integration of hydrodynamics, chemical, and food web parameters. Moreover, Delta Smelt have become so rare that we did not consider it reasonable to try to measure their specific responses, particularly when the action was focused on just a portion of their range.

MATERIALS AND METHODS

Study Area

The focus of this study was the North Delta of the upper San Francisco Estuary (Figure 1). The northernmost region of the study area includes the Colusa Basin–Ridge Cut Slough and extends southward to the lower Sacramento River, with key regions in between such as the Yolo Bypass (upper and lower) and CSC (Figure 1). As mentioned previously, the CSC is a freshwater tidal habitat that includes channels, sloughs, and open water, all of which influence the food web and native fish habitat. The region's complexity is enhanced by the connection of CSC to the Yolo Bypass, a (24,000-hectare) floodplain and tidal slough that acts as one of the primary flood control systems for the City of Sacramento, California. During winter and spring months, the Yolo Bypass floodplain is commonly wetted from both the Sacramento River (by the overtopping of Fremont Weir) and additional west-side tributary inputs, with positive (downstream) outflows to CSC; however, during the drier summer and fall (July to September), the wetted floodplain portion of the bypass is reduced to the small Toe Drain (a perennial riparian canal), which is heavily used to supply water for agriculture and migratory waterfowl habitat (Sommer et al. 2001). With water use exceeding supply to the Toe Drain, summer flow in the Toe Drain is often net negative (upstream) as water moves northward; however, flows in fall become moderately positive (downstream) again, with increased agricultural return water discharge from local and upstream rice-field harvest (Figure 1). Furthermore, diversions from the Toe Drain, North Bay Aqueduct, additional evaporation, and other local

https://doi.org/10.15447/sfews.2021v19iss3art3

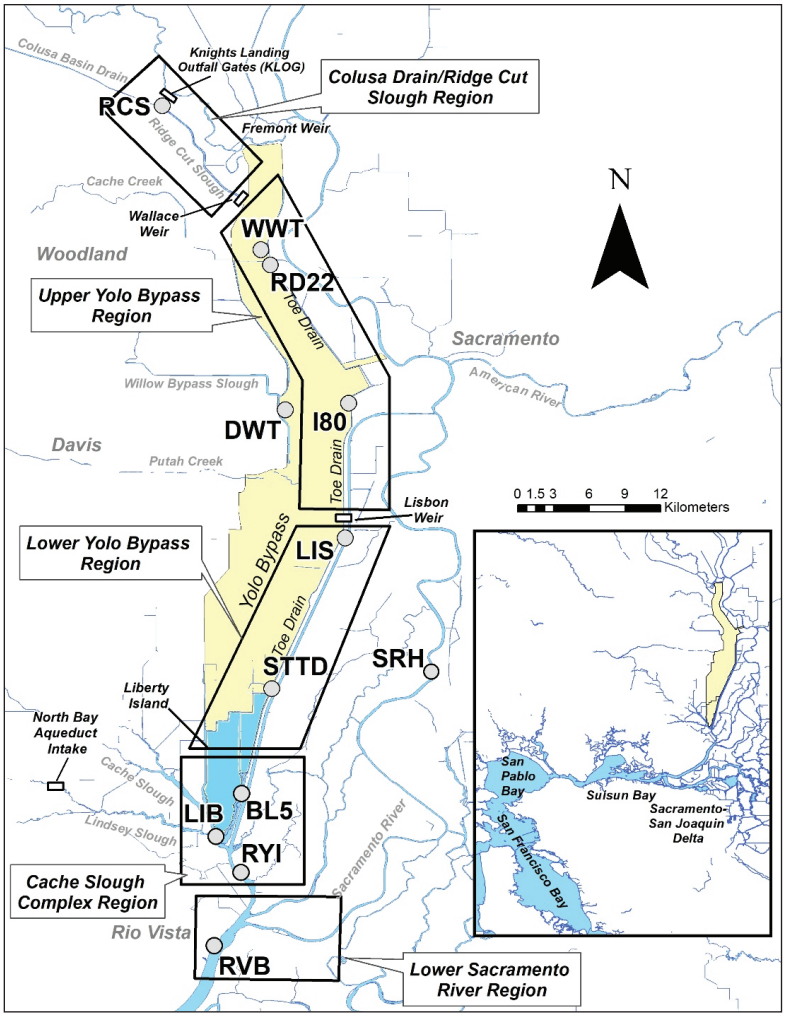

Figure 1 Map of the Yolo Bypass and Delta with water sampling stations, wastewater treatment discharge sampling locations, and the sampling locations with continuous water quality monitoring. Sites include Ridge Cut Slough at Hwy 113 (RCS), Woodland Wastewater Treatment (WWT), Toe Drain at Road 22 (RD22), Davis Wastewater Treatment (DWT), Toe Drain at I80 (I80), Toe Drain below Lisbon Weir (LIS), Screw Trap at Toe Drain (STTD), Prospect Slough (BL5), Liberty Island (LIB), Cache Slough at Ryer Island (RYI), Sacramento River at Rio Vista (RVB), and Sacramento River at Hood (SRH). The San Francisco Estuary is shown in the *inset panel*. The estuary represents the area from the Golden Gate Bridge upstream to Sacramento in the north, and Stockton to the southeast. The Delta portion of the estuary includes the area upstream of Suisun Bay. For the purposes of our study, we considered the North Delta to be the area north of Rio Vista, which includes the labeled Upper Yolo Bypass, Lower Yolo Bypass, Cache Slough, and Lower Sacramento River regions.

consumptive use in the CSC are greater than the upstream inflows during summer, resulting in a net upstream flow from Cache Slough into the CSC. This study used (i.e., repurposed) existing infrastructure for agriculture and flood management activities in the described study area to generate a flow pulse down the Toe Drain during summer. Furthermore, the occurrence of this study during a single year limits its application to other years as a result of natural variation in hydrology and climate in California, but the Yolo Bypass has little change from year to year in July because of the consistent hydrology and land uses during the summer and fall.

Managed Flow Pulse

In July of 2016, the California Department of Water Resources (CDWR) worked with federal and state agencies, irrigation and reclamation districts, and land-owners to generate a larger-than-normal summer flow pulse in the study area by supplementing outflows with additional upstream pumping of water from the Sacramento River into the Colusa Basin Drain (CBD) and Toe Drain. The flow pulse target was to emulate beneficial flow pulse conditions observed in the Yolo Bypass that were similar in the summer and fall of 2011 and 2012 (Frantzich et al. 2018) with a measured discharge of 30 million m^3 (22 taf in 2011) and 33.6 million m^3 (27 taf in 2012), and a maximum daily average net flow rate > 300 cfs at Lisbon Weir (LIS). Although 2 to 4 weeks of net positive flow in the Yolo Bypass was targeted, operations were limited to a 2-week window because of external construction needs. To reach the flow pulse target, we required operational changes by the US Bureau of Reclamation at Keswick Dam to modify water releases to increase

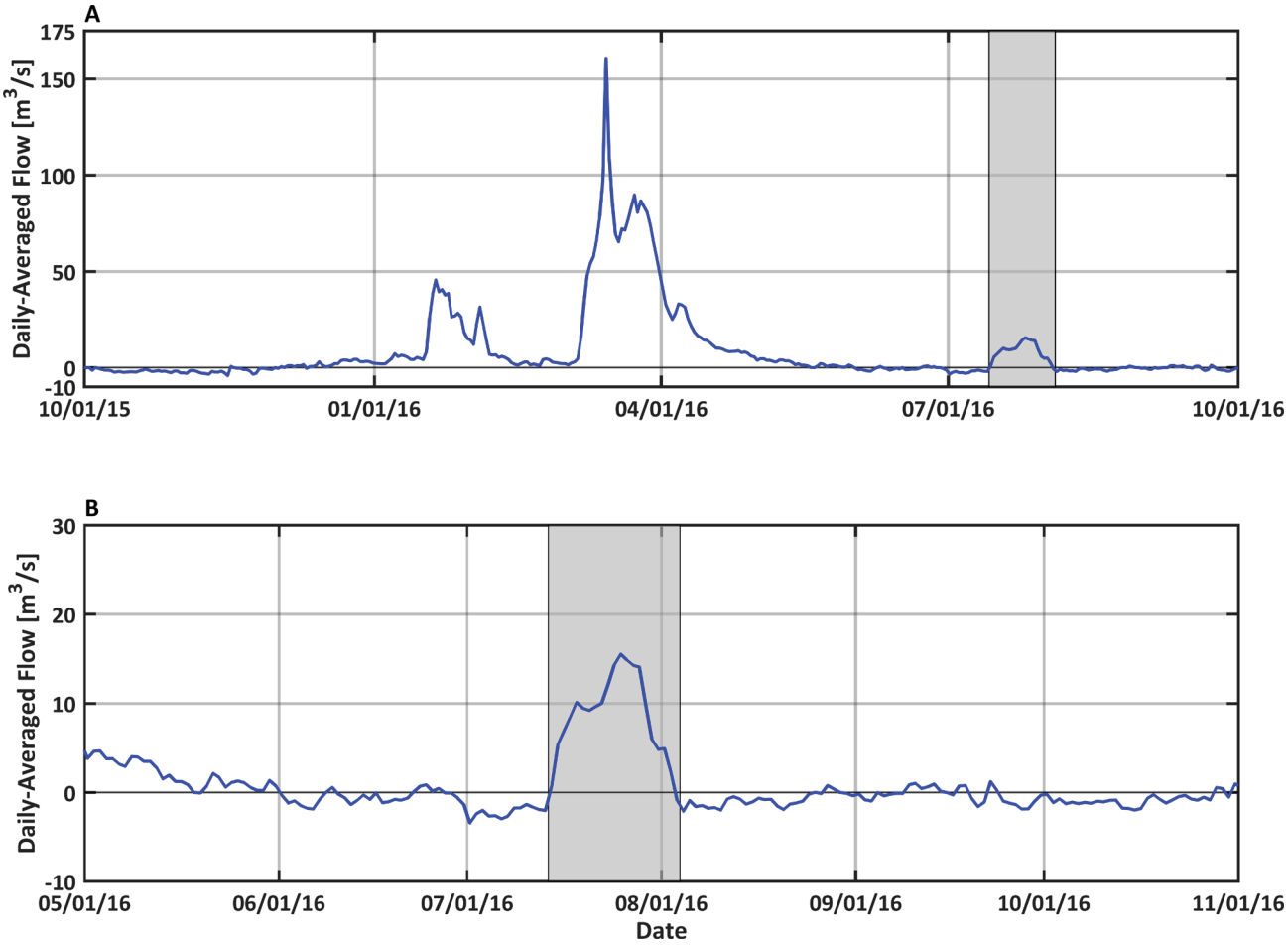

Figure 2 Observed daily-averaged flow through the Toe Drain past Lisbon Weir for (**A**) water year 2016 and (**B**) the summer low-flow period of 2016 around the flow pulse. *Shading* denotes the flow pulse period.

the stage of the Sacramento River. The river stage increase enabled Glenn Colusa Irrigation District and both Reclamation Districts 108 and 2035/Conaway Ranch to divert Sacramento River flow into the CBD and Toe Drain (Figure A1). This was followed by weir operational changes at land-owner properties along the Toe Drain to ensure the flows were not impeded. Lastly, the CDWR Knights Landing Outfall gates (KLOG) were operated at a higher elevation to allow for additional upstream flows to be diverted into Ridge Cut Slough, through the Wallace Weir, and downstream into the Yolo Bypass. Together, operations conveyed and diverted just over 18.5 million m^3 (15 taf), with a total estimated net discharge volume in Yolo Bypass (measured at LIS) of 15.7 million m^3 (12.8 taf) and a maximum daily average net flow of 546 cfs from July 11 to August 1. This net discharge volume was roughly half of the initial flow pulse target during a 2-week period. Operational pumping rates and discharge volumes are summarized in Appendix A (Table A1).

Available field data did not allow for the direct evaluation of how the flow pulse affected hydrodynamics in the CSC, so the high-resolution 3-D UnTRIM San Francisco Bay–Delta Model was used to predict water flow and tracer transport through the estuary, with increased focus on the North Delta study area (MacWilliams et al. 2015). This hydrodynamic modeling was conducted to directly predict the effects of the flow pulse on the hydrodynamics and tracer transport through the CSC and further downstream. The UnTRIM model extends from the Pacific Ocean to the

https://doi.org/10.15447/sfews.2021v19iss3art3

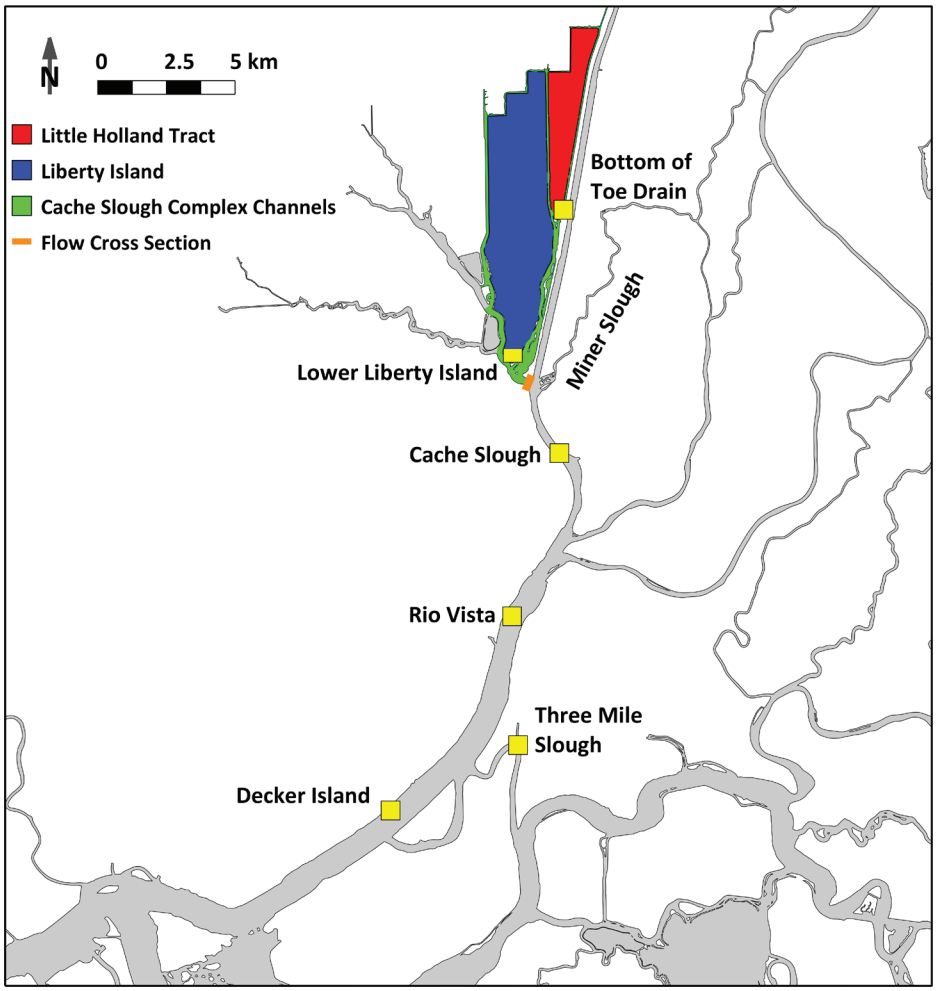

Figure 3 Locations used for evaluating the hydrodynanmic model simulations (*yellow squares*), areas of Little Holland Tract, Liberty Island, and Cache Slough Complex Channel water, and location of Miner Slough

Delta, with increasing grid resolution in smaller channels, resulting in more than 1.4 million 3-D grid cells (Anchor QEA 2020). To increase model resolution and accuracy for the present study, the UnTRIM model grid was refined in the CSC to resolve bathymetry features (e.g., levee breeches, deep channels, stair-step channels) needed to correctly model the routing of flow pulse water from below Lisbon Weir (LIS) through Liberty Island (LIB) (bathymetry data acquired from Wang and Ateljevich [2012]). The model was calibrated using available flow, water level, and specific conductance (converted to salinity) time-series data in the Yolo Bypass and CSC, and has been extensively validated (MacWilliams et al. 2015; MacWilliams and Gross 2007).

Model simulations incorporated observed daily averaged flow, salinity, and water temperature in the Toe Drain as inputs to capture the conditions most accurately at the model boundary in the Toe Drain at LIS. When the flow at LIS is negative, the model boundary acts as a sink of water, resulting in a net upstream flow into the Toe Drain. We used simulations to determine the age, movement, and fate of water masses that originated from the flow pulse, CSC, and downstream (Figure 3). We made one simulation based on historical conditions with the observed flows past LIS during the 2016 flow pulse. An additional simulation was made with the flow pulse removed (Figure 4A), but was otherwise identical to the historical conditions. Comparing these two simulations allowed us to examine how the flow pulse affected water age and movement. For the model simulation without a flow pulse, a linear interpolation from just before to just after the flow pulse was used to estimate the water flow

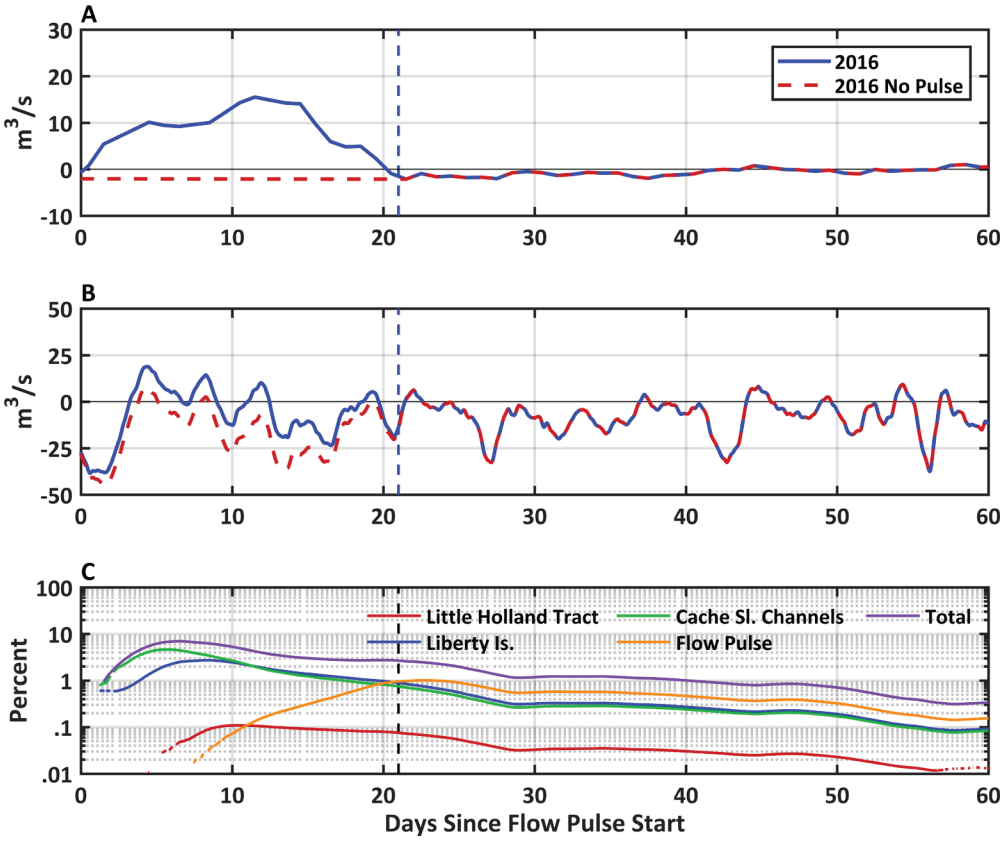

Figure 4 (**A**) Observed daily-averaged flow past Lisbon Wier during the 2016 flow action (*blue*) and corresponding flow used in model simulations for the no flow action scenario (*red*); (**B**) predicted tidal average flow out of CSC; (**C**) predicted percent of water from different sources at Rio Vista for the simulation including the flow pulse

at LIS (Figure 1). After the model spin-up period, each simulation included 1 month before the flow pulse and 3 months after the flow pulse.

We analyzed water age (Deleersnijder et al. 2001; Delhez et al. 1999) at six locations (Bottom of Toe Drain, LIB, CSC, RVB, Sacramento River at Decker Island, and Three Mile Slough; Figure 3) to determine the average time elapsed (in days) since the flow pulse water at a given location passed LIS, with flow pulse water set to age 0 days when it entered the model domain at LIS. For example, at 1 day into the flow pulse, the flow pulse water at the leading edge is given age 1 day, and water that passed LIS just before is given age 0 day. We performed tracer analysis (similar to using a dye or tagging water) on five water masses (flow pulse, Miner Slough, and three CSC sub-areas, see Figure 3), to determine the percentage of water that originated from the flow pulse at a given location, as well as to track other water masses during and after the flow pulse. We did not calculate water age for the three CSC sub-areas because there is no continuous supply of new water, so the age given would be uniform everywhere, and be simply the number of days elapsed since the start of the flow pulse.

We also used hydrodynamic model simulations to predict the flow of water between the CSC and downstream regions because no observations of flow at this location were available. We extracted predicted flow from the hydrodynamic model at the cross-section between CSC and Cache Slough shown on Figure 3. The tidal flow of water between the CSC and Cache Slough varies from about $-1{,}800\ m^3\ s^{-1}$ to $1{,}800\ m^3\ s^{-1}$ (Figure A2). Because the tidal flows are so large in relation to the magnitude of the flow pulse, it is very difficult to visualize how the flow pulse affects the instantaneous flows. After tidal averaging over 24.8 hours, flow between the CSC and Cache Slough varies from about $-60\ m^3 s^{-1}$ to $30\ m^3\ s^{-1}$ during low-flow periods; the effect of the flow pulse on tidally averaged flows is evident (Figure 4B).

https://doi.org/10.15447/sfews.2021v19iss3art3

Water Quality and Plankton Monitoring

Our basic approach was to monitor water quality and plankton before, during, and after the flow pulse. The study design included sample collection at multiple locations along a north-to-south transect, following the path of the flow pulse through Yolo Bypass and downstream to the Sacramento River (Figure 1). We collected water quality and biological samples weekly from June through September 2016 ($n = 5$ to 11 samples per site) along a north-to-south transect from the upper Yolo Bypass at Ridge Cut Slough (RCS) south to the Rio Vista Bridge (RVB) on the lower Sacramento River. The sampling transect was divided into five distinct regions based on differences in key habitat attributes between sites (Figure 1). Regions included: (1) Colusa Drain /Knights Landing Ridge Cut, (2) upper Yolo Bypass, (3) lower Yolo Bypass, (4) CSC, and (5) the lower Sacramento River. The sites within these regions included Ridge Cut at Highway 113 (RCS), Woodland Wastewater Treatment Discharge (WWT), Toe Drain at County Road 22 (RD22) Davis Wastewater Discharge (DWT), Toe Drain at Interstate 80 (I80), LIS, Screw Trap at Toe Drain (STTD), Prospect Slough (BL5), LIB, Cache Slough at Ryer Island (RYI), and lower Sacramento River at Rio Vista Bridge (RVB). The Sacramento River at Decker Island and Three Mile Slough were not sampled for water quality or biological constituents; they were only used for hydrodynamic modeling analyses. Two separate field crews sampled sites on the same day during the mid-morning, and all samples were collected within 24 hours of each other.

Water samples were collected near the surface (≤ 1 m) at each site ($n = 10$ to 11 per site, except RCS $n = 5$) for later laboratory analysis of chlorophyll *a* (an indicator of phytoplankton biomass), nutrients, and phytoplankton enumeration. After field collection, water samples were stored on wet ice (4 °C) until the samples were filtered or preserved later that day. The next sections describe specific field and laboratory collection methods for water quality and plankton.

Water Quality

Discrete measures of water temperature (°C), specific conductance (μS cm^{-1}), pH, and dissolved oxygen (DO, mg L^{-1}) were collected at each site using a Yellow Springs Instruments (YSI) EXO 556 multi-parameter handheld instrument. Turbidity (NTU) was measured using a HACH 2100Q Portable Turbidity meter. Light irradiance (mole quanta $m^{-2} day^{-1}$) was measured through vertical profiles at four depths determined by 75%, 50%, 25%, and 1% of surface irradiance, using a LI-COR 193SA spherical quantum sensor at integrated depth intervals.

Continuous water quality data for total chlorophyll fluorescence and specific conductance were collected at 15-minute intervals using YSI 6600 V2 multi-parameter sondes at fixed depths. Sondes were deployed during the study period at four sites from Ridge Cut Slough (RCS) to the base of the Toe Drain at STTD (Figure 1). Additional, continuous water quality data were acquired from the CDWR Division of Environmental Services YSI at lower Sacramento River at Rio Vista Bridge (RVB) (*http://cdec.water.ca.gov/dynamicapp/QueryF?s=RVB*) and US Geological Survey's YSI from a station at the base of LIB in the CSC (*https://waterdata.usgs.gov/nwis/qw*). Flow, velocity, and stage measurements for the Yolo Bypass were obtained from gauges operated by the CDWR at LIS (*http://cdec.water.ca.gov/dynamicapp/QueryF?s=LIS*). The CDWR used an acoustic Doppler current profiler (ADCP) and cross-sectional channel depth measurements to estimate the volume of flow pulse discharge at LIS from July to August.

All continuous CDWR water quality data for sites RCS, RD22, I80, LIS, and STTD were examined for validity, and for outliers using KISTERS Hydstra software (*http://kisters.com.au/hydstra.html*). In the KISTERS Hydstra software, specific conductance data have a maximum allowable limit of > ± 5% difference between lab standards and the water quality sonde reading. Chlorophyll has a maximum allowable limit of > ± 4 $\mu g L^{-1}$ difference between 0 $\mu g L^{-1}$ standard and the sonde reading. Dissolved oxygen data have a maximum allowable limit of > ± 0.8 $mg L^{-1}$ difference between a 100%

saturation DO concentration standard (related to temperature, atmospheric pressure, and salinity) and the sonde reading. If the total deviation for a given deployment period is greater than this maximum allowable limit, then the observation was removed. This resulted in less than 5% of data being removed for all sites, except for STTD that had 15% of DO data removed because of heavy biofouling. The calibration criteria for the continuous-water quality sondes are based on established methods by USGS in Wagner et al. (2006). The CDWR data from site RVB and USGS data from site LIB were further examined for validity and for outliers using three primary modified tests: gross range, spike, and rate of change tests as referenced in the US Integrated Ocean Observing System (IOOS 2020). These outlier detection procedures resulted in the removal of less than 10% of 15-minute data values from the RVB and USGS sites.

To further determine the potential responses to the flow pulse in algal growth (i.e., photosynthesis), a DO saturation concentration time-series was calculated using computation methods recommended by Benson and Krause (1984). The actual measured time-series DO ($mg\,L^{-1}$) was then compared to the calculated DO saturation concentration to evaluate the occurrence of potential photosynthetic DO from algal production. The measured total chlorophyll fluorescence was further used to associate changing algal biomass with DO trends.

Nutrients

Water samples from each site were filtered in the laboratory in preparation for quantification of nutrients such as nitrate + nitrite ($NO_3 + NO_2$), ammonium (NH_4), ortho-phosphate (PO_4^{3-}), silica ($Si(OH)_2$), and dissolved organic carbon (DOC). Nutrient samples were filtered through 0.45-µm filters (Millipore HATF04700), which were then immediately frozen at –20 °C. Ambient nutrient concentrations were analyzed using various established US EPA and American Public Health Association (APHA) analysis methods: $NO_2 + NO_3$ (Std. Method 4500-NO3-F Modified), NH_4 (EPA 350.1), PO_4 (EPA 365.1), $Si(OH)_2$ (EPA 200.7D), DOC (EPA 415.3), and dissolved inorganic nitrogen (DIN) ($NO_3 + NO_2 + NH_4$). Analyte determination (n = 10 to 11 per site, except n = 5 for RCS) was conducted at the CDWR Bryte Laboratory, West Sacramento, California.

Chlorophyll and Phytoplankton

In tandem with water filtration for nutrient analytes, samples were collected for chlorophyll *a* and phytoplankton (n = 10 to 11 per site). Concentrations of chlorophyll *a* were acquired from the extraction of pigments on glass-fiber filters (47 µm Millipore) with 90% aqueous acetone and using spectrophotometry (Standard Method 10200H, APHA [2012]). An additional sample of site water (50 mL) was preserved in an amber glass vial with 4% Lugol's solution until later identification, enumeration, and measurements were taken of cell dimensions for the phytoplankton species collected (conducted by BSA Environmental Inc., Beechwood, OH). Phytoplankton composition was determined and enumerated to at least the genus level using the Utermöhl microscope method (Utermöhl 1958) from samples collected at site LIS. Phytoplankton samples were counted for at least 400 total algal units, with 100 units of the dominant taxa. Length measurements were recorded on the first 25 units of major phytoplankton taxa, and the first five units of minor taxa to calculate biovolume ($\mu m^3\,mL^{-1}$) from formulas given for different algal shapes by Keller et al. (1980). The biomass in $\mu g\,L^{-1}$ – C was calculated using carbon-to-volume (C:vol) relationships from (Menden–Deuer and Lessard 2000). This included using the established C:vol relationship for diatoms of $pgC\ cell^{-1} = 0.288 \times (\text{biovolume-}\mu m^3\ L^{-1})^{0.811}$ and for all other taxa groups as $pgC\ cell^{-1} = 0.216 \times (\text{biovolume-}\mu m^3\,L^{-1})^{0.939}$.

To estimate changes in phytoplankton food quality for secondary consumers before, during, and after flow pulses, we adopted methods used by Galloway and Winder (2015). They performed a thorough literature review of available long-chain essential fatty acid (LCEFA) profiles for the most prevalent algal taxa, and generated a food-quality index for broader algal groups based on fatty acid % (FA%): chlorophytes, cryptophytes, cyanobacteria, diatoms, dinoflagellates, and

https://doi.org/10.15447/sfews.2021v19iss3art3

haptophytes. We applied the average € LCEFA % dry weight (DW) content for each algal group established in Galloway and Winder (2015). We further calculated the algal-derived average concentrations of % LCEFA µg L^{-1} for our phytoplankton data set to establish food quality using the equation:

€ µg FA category L^{-1} = € µg biomass AGi * (average AGi FA % DW/100), (1)

where, for the fatty acid category € LCEFA, the total calculated € µg FA L^{-1} is the sum of the calculated total biomass (µg C L^{-1}) across the major algal groups in our phytoplankton data set, multiplied by the average fatty acid content of the algal group (AGi). The AGi FA% DW was then divided by 100 to express as a proportion before being multiplied by the AGi biomass.

Zooplankton

A single zooplankton sample was collected by boat at each site with a conical plankton net (0.50 m mouth, 2 m length, and 150 µm mesh) held just under the water surface and towed near the center of the channel for approximately 3 to 5 minutes during the mid to late morning on an ebb tide. Zooplankton samples were concentrated into a 1L Nalgene bottle and preserved in 10% formalin. Note that demersal vertical migration of some adult copepods has been documented to occur during the day in this region (Kimmerer et al. 2018), and this behavior could result in our sampling under-representing these zooplankton. We calculated the sample volume using General Oceanic's Model 2030R flow meters mounted in the mouth of the net. To address varied sampled water volumes across sites, we calculated a zooplankton catch-per-unit-volume (CPUE) or number of taxon per cubic meter of water filtered. The CPUE for zooplankton taxon collected in our net was calculated using the following equation:

CPUE (or the number of taxon per cubic meter of water filtered) = [(C/S)L]/V, (2)

where, the cumulative number of taxon counted for the sample (C) is divided by the number of Sedgewick–Rafter cells examined (S) multiplied by the reconstituted sample volume (dilution volume) in milliliters (L). This total is then divided by the volume of water filtered through the net in cubic meters (V).

Zooplankton identification and quantification (n = 6 to 7 per site) were conducted by BSA Environmental Inc., Beechwood, OH. Zooplankton samples were sub-sampled to target up to a total count of 250 mesozooplankton and 300 microzooplankton per sample. Samples were examined under a compound microscope at a minimum of 100x magnification to identify taxa to at least the genus level, with taxonomic resolution dependent on species and life stage.

Statistical Analyses

To determine the effect of the flow pulses on habitat changes of physical, chemical, and biological conditions (i.e., water quality, chlorophyll, and nutrients), we used a one-way analysis of variance (ANOVA). Because of limited statistical power to test interactions between independent variables of flow-pulse period and region, a series of ANOVAs were conducted separately; first to test effects of flow pulse period (i.e., before, during, and after) within each region, and second to test the differences between regions within each pulse period. We used the Tukey method after ANOVA tests to identify which regions grouped together by mean before, during, and after the flow pulse event. All data were log10(x)-transformed before the ANOVA and Tukey test analyses were run. The dependent variables included: water temperature (°C), specific conductance (µS cm^{-1}), turbidity (NTU), chlorophyll *a* (µgL^{-1}), NH_4 (µM-N), NO_3 + NO_2 (µM-N), PO_4^{3-} (µM-P), Si $(OH)_2$ (µM-Si), DIN (µM-N), and DOC (µM).

Phytoplankton genera biomass as biovolume was square-root-transformed and analyzed using analysis of similarities (ANOSIM) to determine the strength of separation (ANOSIM R) and significant difference in biomass before, during, and after the flow pulse. We used the non-parametric ANOSIM analysis as an alternative to a one-way ANOVA because of the non-normal distribution of the square-root-transformed phytoplankton

biomass data. A similarity percentage analysis (SIMPER) was then used on the phytoplankton biomass data to determine the total dissimilarity between communities and the contribution of the most discriminating phytoplankton genera to the dissimilarity before, during, and after flow pulses. Non-metric multi-dimensional scaling (NDMS) was conducted on the square-root transformed data for the lower Yolo Bypass, CSC, and lower Sacramento River regions using the Bray–Curtis Similarity Resemblance Matrix with overlayed vectors for phytoplankton taxa based the Pearson correlation of ≥ 0.7. NMDS analysis are provided in Appendix A.

Zooplankton taxa group density or CPUE (number m^{-3}) data were square-root-transformed for sites in the lower Yolo Bypass, CSC, and lower Sacramento River regions. Pearson correlation analysis was completed for both Toe Drain below Lisbon Weir flow and site-specific chlorophyll-*a* concentration as separate independent variables to calculate based on 40 sample observations for each of the primary zooplankton taxa groups: calanoid copepods, cyclopoid copepods, and cladocerans as the dependent variables. These correlations were used to determine any significant relationships between changing flow conditions and phytoplankton biomass on the local zooplankton communities. Similar to phytoplankton biomass data, square-root-transformed zooplankton abundance data were analyzed using ANOSIM to determine the ANOSIM R and significant difference in biomass before, during, and after the flow pulse. SIMPER was then used on the zooplankton data to determine the total dissimilarity between communities and the contribution of the most discriminating zooplankton genera to the dissimilarity before, during, and after flow pulses. NDMS was conducted on the square-root transformed data for the lower Yolo Bypass, CSC, and lower Sacramento River regions using the Bray–Curtis Similarity Resemblance Matrix with overlayed vectors for zooplankton taxa based on the Pearson correlation of ≥ 0.7. NMDS analyses are provided in Appendix A.

We completed the univariate statistical analyses (ANOVA and Tukey test) using Minitab 16 software (Minitab 16 Statistical Software 2010), and computed the multivariate analysis (ANOSIM and SIMPER) using PRIMER-E version 7 software (Primer-e v7 2015).

RESULTS

Managed Flow Pulse

Flow conditions at LIS before the summer flow pulse followed the typical seasonal trend, with net flow being predominantly net negative (upstream after tidal influence was removed) from local water withdrawal by early June (Figure 2). However, the net flow at LIS switched southward during the flow pulse with net positive flow downstream. The flow pulse maintained relatively high flow past Lisbon Weir, with an average of 9.1 $m^3 s^{-1}$ (321 cfs) during the flow pulse, a maximum daily average net flow of 15.5 $m^3 s^{-1}$ (546 cfs) at LIS (Figure 4A), and continuous flow into the CSC. In the simulation with the flow pulse removed, the model predicted a net northward transport of water through the Toe Drain past Lisbon Weir during the entire flow pulse period, with net flows only becoming southward about 45 days after the start of the flow pulse period (Figure 4A). This indicates that the flow pulse resulted in a reversal in the net flow direction through the Toe Drain past Lisbon Weir for a prolonged period of time.

With the flow pulse, predicted net flows from CSC to downstream regions remained predominantly northward (negative, into the CSC) when averaged over the flow pulse period at – 3.1 $m^3 s^{-1}$ (– 110 cfs) (Figure 4B). The predicted net flow into the CSC when averaged over the complete duration of the flow pulse resulted from the magnitude of the flow pulse not being large enough to exceed the intakes and diversions in the CSC and produce an averaged flow out of the CSC, when averaged over the entire duration of the 2016 flow pulse. However, there were periods of predicted net flow out of the CSC during the flow pulse (Figure 4B and Figure A2). Without the flow pulse, the predicted net flow was only directed south out of the CSC for a few very short-duration, low-magnitude periods, and was directed more into

https://doi.org/10.15447/sfews.2021v19iss3art3

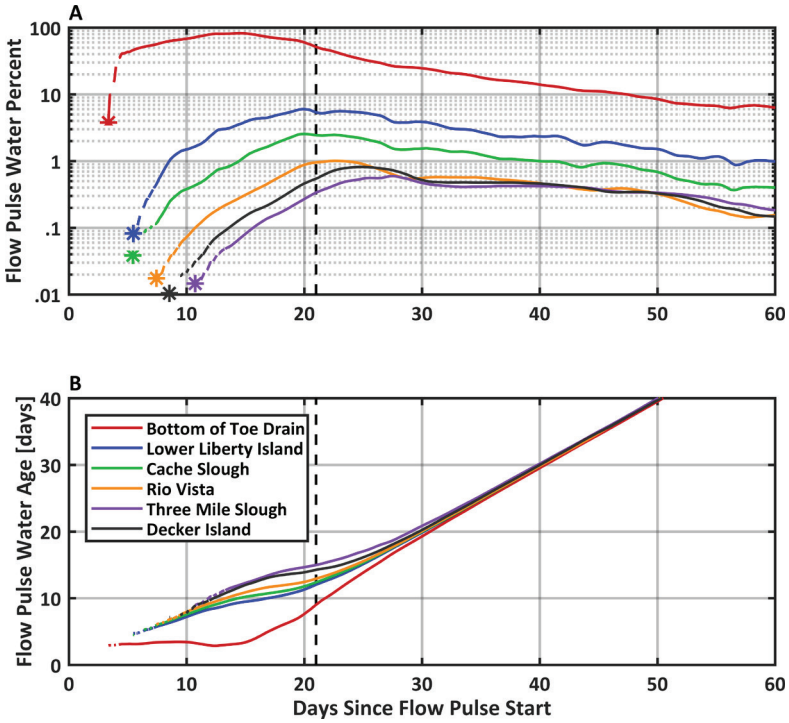

Figure 5 Predicted tidal-averaged (**A**) flow pulse water percent and (**B**) flow pulse water age (days) across sites based on the UnTRIM simulation including the flow pulse. The *dashed vertical line* indicates the end of the flow pulse. *Asterisks* indicate the first day the pulse water appeared at each location. Water age is the average amount of time elapsed since the flow pulse water at a given site passed Lisbon Weir.

the CSC than in the simulation with the flow pulse. Overall, the flow pulse increased the predicted net flows out of the CSC to downstream regions and decreased the predicted net flows into the CSC.

Simulations that included the flow pulse indicated that flow pulse water initially reached the bottom of the Toe Drain near the connection with CSC within 3 days after the pulse began, the southern end of LIB and Cache Slough in 5 days, and Rio Vista in 7 days (Figure 5A). The percent of the flow pulse water at the bottom of the Toe Drain increased to nearly 100% of the water at the bottom of the Toe Drain (Figure 5A), but the percent flow pulse water did vary, depending on the tides. Downstream regions, including LIB, CSC, and Rio Vista, had substantially lower percent flow pulse water, peaking at 1% to 6% (Figure 5A), with greater tidal variation than at the bottom of the Toe Drain. The average age of the flow pulse water at the bottom of the Toe Drain, which is the average amount of time elapsed since the flow pulse water passed LIS, remained less than about 6 days, until about 15 days after the start of the flow pulse, when the water age began to gradually increase (Figure 5B). This start of the gradual increase in age corresponded to the decline in the magnitude of the flow pulse. The average flow pulse water age at LIB, CSC, and Rio Vista was larger than at the bottom of the Toe Drain, indicating that the flow pulse water took a longer amount of time to transit through those sites (Figure 5B).

Although the flow pulse only increased the net outflow (southward) from CSC by a moderate amount relative to the weekly variability in the tidal-average flow, when compared to predicted conditions if the flow pulse had not occurred (Figure 4B), southward transport of water masses from Little Holland Tract, LIB and CSC channels to Rio Vista were evident (Figure 4C; Figures A3, A4). Although the flow pulse did not completely flush out the water from Little Holland Tract or CSC, the flow pulse modified the hydrodynamics and resulted in increased transport of CSC water downstream relative to the conditions which would have existed if the flow pulse had not occurred (Figure A4).

Table 1 Mean (±SD) discrete physical data and chlorophyll-*a* measurements before, during and after the flow pulse from the following regions (north to south): Colusa Drain-Ridge Cut Slough (site RCS), Upper Yolo Bypass (sites RD22, I80), Lower Yolo Bypass (sites LIS, STTD), Cache Slough Complex (sites BL5, LIB, RYI), and Lower Sacramento River (site RVB).

Region	Flow pulse timing	Water temperature (°C)	Specific conductance (µS cm^{-1})	Turbidity (NTU)	Chlorophyll *a* (µgL^{-1})	Light Irradiance (mole quanta $m^{-2}day^{-1}$)
Colusa Drain–Ridge Cut Slough	Before	25.1 (0.8)	781 (137)	30.7 (6.4)	23.7 (10.2)	7.43 (---)
	During	25.8 (1.4)	605 (97)	24.7 (1.8)	12.1 (7.3)	11.75 (---)
	After	---	---	---	---	---
Upper Yolo Bypass	Before	24.1 (2.2)	830 (18)	64.8 (11.8)	34.6 (16.2)	6.74 (0.51)
	During	25.5 (1.0)	644 (170)	57.4 (20.2)	27.0 (24.1)	9.23 (1.03)
	After	22.2 (1.6)	748 (100)	48.8 (10.8)	17.2 (11.0)	7.18 (1.07)
Lower Yolo Bypass	Before	23.8 (2.4)	258 (115)	63.5 (7.0)	11.3 (5.3)	9.18 (1.04)
	During	24.4 (1.3)	469 (223)	56.3 (20.6)	16.7 (7.2)	9.91 (0.77)
	After	22.0 (1.4)	310 (115)	60.7 (24.4)	12.7 (3.6)	9.25 (2.49)
Cache Slough Complex	Before	21.9 (1.2)	136 (19)	27.4 (19.5)	8.4 (5.4)	21.05 (8.74)
	During	22.5 (1.6)	159 (74)	22.0 (17.3)	12.1 (5.6)	22.52 (6.53)
	After	20.7 (1.3)	163 (23)	10.4 (8.2)	6.7 (5.0)	23.94 (6.12)
Lower Sacramento River	Before	22.4 (1.3)	121 (10)	12 (4.5)	7.0 (3.4)	27.86 (1.53)
	During	22.3 (0.9)	113 (1)	6.7 (2.6)	4.5 (0.28)	33.22 (---)
	After	21.3 (0.7)	146 (17)	4.6 (1.1)	8.1 (6.3)	32.65 (0.68)

a. "---" Indicates data not sampled.

WATER QUALITY AND PLANKTON MONITORING

Water Quality

Discrete physical water measurements collected throughout the five sampling regions (Figure 1) during the 2016 study period are summarized in Table 1. The mean water temperatures (ranging from 18.2 to 26.7 °C) between regions before the flow pulse were similar (ANOVA; $p > 0.05$), but during and after the pulse temperatures differed (ANOVA $p < 0.05$), with the upper Yolo Bypass region having warmer mean water temperatures (Tukey test; $p < 0.05$) than the other regions. Specific conductance and turbidity differed between regions (ANOVA $p < 0.05$). The upper regions of the study area are surrounded by agricultural diversions, and subsequent water quality is affected by local water intakes and discharges that raise the specific conductance and alter turbidity conditions. Turbidity was highest in the upper and lower Yolo Bypass throughout the entire study period (Tukey test; $p < 0.05$), whereas the Colusa Drain–Ridge Cut Slough and upper Yolo Bypass had the highest specific conductance throughout the flow pulse—and were significantly higher than other regions (Tukey test; $p < 0.05$) before and after the flow pulse. The specific conductance increased during the flow pulse as upstream water sources exchanged with the lower sites, which caused the mean values in the lower Yolo Bypass not to differ significantly (Tukey test; $p > 0.05$) from the Colusa Drain–Ridge Cut and central Yolo Bypass regions. Continuous monitoring sites from Colusa Basin-Ridge Cut Slough to the CSC regions (Figure 6) also recorded increases in specific conductance with flow pulse at downstream sites. Water column light irradiance data within the four regions tracked closely with turbidity, as lower levels were measured in the upper study regions and higher levels in the downstream CSC and lower Sacramento regions (Table 1). In addition, increased light irradiance levels in the upper study regions were observed to be associated with the flow pulse.

https://doi.org/10.15447/sfews.2021v19iss3art3

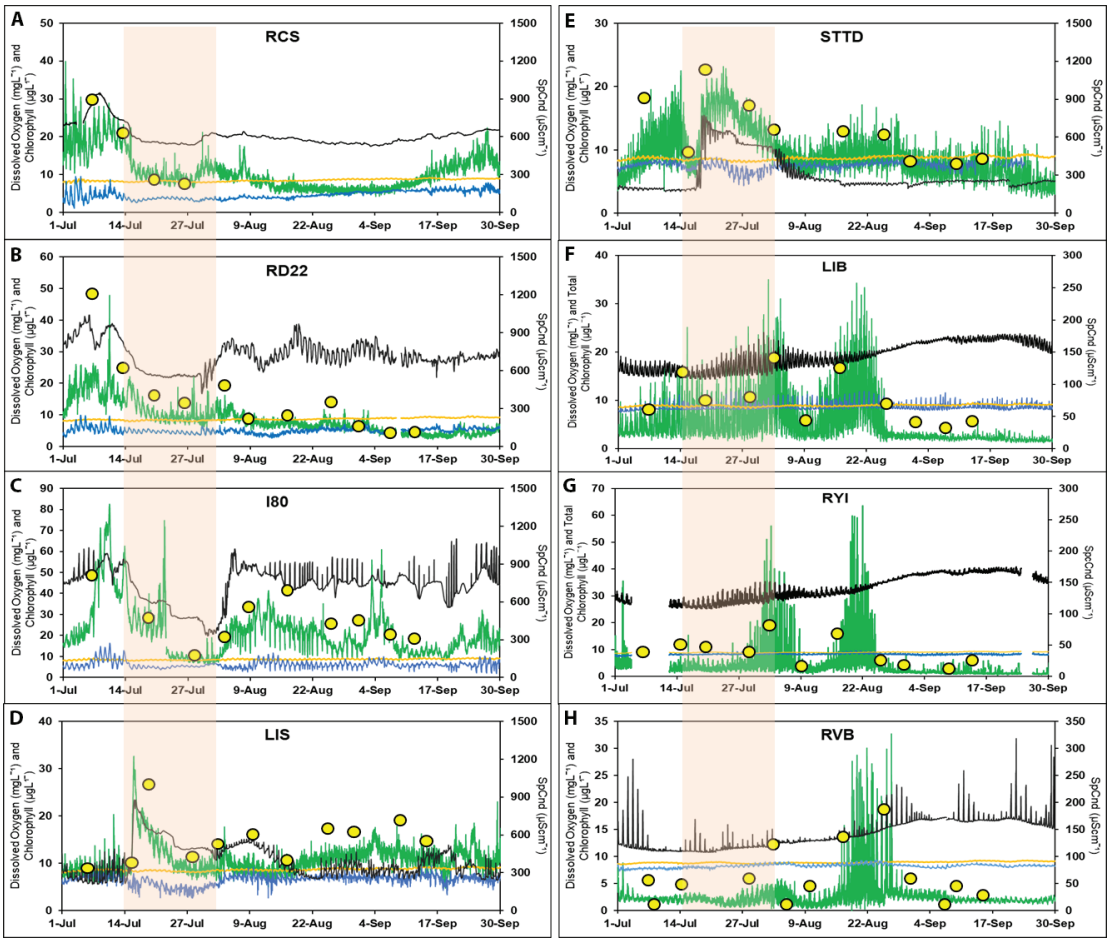

Figure 6 Continuous water quality and flow time series data by site. The left *y*-axis represents total chlorophyll fluorescence (µg L^{-1}, *green line*), discrete chlorophyll-*a* concentration (µg L^{-1}, *yellow points*), dissolved oxygen (mg L^{-1} *blue line*), and dissolved oxygen saturation point (*orange line*). The right *y*-axis is specific conductance (µS cm^{-1}, *black line*). The *shaded area* represents the flow pulse July 14-August 1. **Y*-axis unit scales vary by site. Sites are presented in order from north to south (**A-H**) spanning across regions; Colusa-Drain/ Ridge Cut Slough (site RCS [**A**]); Upper Yolo Bypass (sites RD22 [**B**], I80 [**C**]), Lower Yolo Bypass (sites LIS [**D**], STTD [**E**]), Cache Slough Complex (sites LIB [**F**], RYI [**G**]), and Lower Sacramento River (site RVB [**H**]).

Nutrients

DIN, PO_4, $Si(OH)_4$, and DOC concentrations were significantly different among regions over the course of our study (ANOVA $p < 0.05$). The lowest nitrogen concentrations and N:P ratios were in the Colusa Basin–Ridge Cut Slough and lower Yolo Bypass regions (Table 2). The highest concentrations of $NO_3 + NO_2$, PO_4, and $Si(OH)_2$ were observed in the upper Yolo Bypass (Table 2). This region is subject to substantial loading of nutrients from both the Woodland, California (site WWT) and Davis, California (site DWT) wastewater treatment plant discharges (Frantzich et al. 2018). The $NO_3 + NO_2$ concentrations from site WWT were exceptionally high, with mean concentrations of 109 µmM-N and a max concentration of 203 µmM-N. The NH_4 concentrations from site DWT were high, with mean concentrations of 41 µmM-N and a max concentration of 202 µmM-N. Both sites had high levels of PO_4, with WWT at > 84 µmM-P and DWT values > 71 µmM-P. This region showed a significant difference (Tukey test; $p < 0.05$) in both $NO_3 + NO_2$ and PO_4 before and after the flow pulse from other regions, but was not significantly different from other regions during the flow pulse (Tukey test; $p > 0.05$). There was an observed marginal increase of $NO_3 + NO_2$ (Table 2) and a decrease in NH_4 concentrations during the flow pulse in the lower Yolo Bypass. The upper

Table 2 Mean (±SD) nutrient concentrations before, during and after the flow pulse by region. Regions from north to south are Colusa Drain–Ridge Cut Slough (site RCS), Upper Yolo Bypass (sites RD22, I80), Lower Yolo Bypass (sites LIS, STTD), Cache Slough Complex (sites BL5, LIB, RYI), and the Lower Sacramento River (site RVB).

Region	Flow Pulse Timing	NH_4 (µM)	NO_3+NO_4 (µM)	DIN (µM)	PO_4 (µM)	$Si(OH_2)$ (µM)	DOC (µM)	N:P
Colusa Drain-Ridge Cut Slough	Before	1.04 (0.48)	0.14 (0.07)	1.18 (0.41)	2.16 (0.37)	334 (24.7)	712 (53)	0.5 (0.1)
	During	3.27 (0.82)	0.86 (0.19)	3.10 (0.96)	1.09 (0.16)	338 (13.3)	491 (80.3)	4 (1)
	After	---	---	---	---	---	---	---
Upper Yolo Bypass	Before	4.57 (3.64)	8.08 (7.23)	12.65 (6.76)	6.37 (2.13)	316 (27.2)	685 (38.7)	2 (1)
	During	2.05 (0.63)	1.05 (0.56)	3.10 (0.88)	1.83 (0.88)	334 (10.5)	512 (130)	2 (1)
	After	6.57 (4.66)	13.58 (11.69)	20.15 (10.48)	9.86 (4.28)	388 (22.3)	536 (138)	2 (1)
Lower Yolo Bypass	Before	1.86 (1.42)	0.37 (0.23)	2.23 (1.53)	1.05 (0.36)	113 (22.5)	289 (65)	2 (1)
	During	1.03 (0.37)	0.42 (0.30)	1.45 (0.47)	1.28 (0.43)	247 (103)	411 (156)	1 (0.4)
	After	2.65 (4.00)	0.29 (0.40)	2.95 (3.98)	1.23 (0.42)	233 (90)	300 (63.5)	3 (4)
Cache Slough Complex	Before	6.21 (4.63)	1.22 (0.60)	7.43 (5.15)	0.61 (0.12)	168 (45.9)	175 (26.3)	13 (10)
	During	3.67 (2.79)	0.69 (0.44)	4.36 (3.20)	0.54 (0.17)	160 (40.1)	188 (50.8)	9 (7)
	After	5.20 (4.10)	0.79 (0.46)	5.99 (4.53)	0.70 (0.15)	219 (46.3)	183 (29)	9 (8)
Lower Sacramento River	Before	9.21 (0.97)	1.76 (0.13)	10.97 (1.10)	0.47 (0.07)	206 (5.88)	150 (11.8)	24 (6)
	During	9.22 (1.88)	1.23 (0.05)	10.46 (1.93)	0.42 (0.01)	204 (9.46)	144 (4.81)	25 (5)
	After	8.57 (1.45)	1.41 (0.21)	9.98 (1.60)	0.58 (0.08)	242 (41.5)	153 (8.13)	17 (2)

a. "---" Indicates data not sampled.

regions also had the highest levels of DOC, with the Colusa Basin–Ridge Cut Slough region having >907 µmM-C. The CSC and lower Sacramento River regions had no significant difference (Tukey test; $p > 0.05$) in mean concentrations of DIN, PO_4, $Si(OH)_2$, and DOC throughout the flow pulse. The lower Sacramento River region had the highest mean NH_4, and N:P ratios were always greater than 10 (Table 2), which indicates that N was not a limiting nutrient during the study period.

Chlorophyll and Phytoplankton

The chlorophyll-*a* concentrations were significantly different (ANOVA $p < 0.05$) among regions before, during, and after the flow pulse. The Colusa Drain–Ridge Cut Slough and upper Yolo Bypass regions had the highest concentrations of chlorophyll *a* throughout the flow pulse (Table 1 and Figure 6). The chlorophyll-*a* concentrations increased during the flow pulse in the lower Yolo Bypass and CSC (Table 1 and Figure 6), with these regions not having a mean difference (Tukey test; $p > 0.05$) from the upstream Colusa Basin–Ridge Cut Slough and upper Yolo Bypass regions. The lower Sacramento River observed a substantial increase in chlorophyll-*a* concentration after the flow pulse, with a max of 19.5 $\mu g L^{-1}$ measured on August 22 (Figure 6).

Continuous total chlorophyll fluorescence ($\mu g L^{-1}$) time-series and discrete grab sample data for chlorophyll *a* showed evidence of high phytoplankton biomass in the Colusa Basin–Ridge Cut Slough and upper Yolo Bypass regions (Figure 6). The total chlorophyll fluorescence data showed an increasing trend in the lower Yolo Bypass during the flow pulse. The chlorophyll was also elevated in the lower Yolo Bypass at site STTD, and in the CSC at site LIB just before the flow pulse, but further increased during the flow pulse (Figure 6). Specific conductance time-series data at the same stations in the Colusa Basin Drain–Ridge Cut Slough, lower Yolo Bypass, upper Yolo Bypass and CSC closely followed the chlorophyll trend, because water sources in the upper regions with higher specific conductance

https://doi.org/10.15447/sfews.2021v19iss3art3

and chlorophyll moved downstream throughout the flow pulse. (Figure 6). Two similar peaks of 30–70 µg L^{-1} in chlorophyll were observed at CSC sites LIB and RYI, with one occurring toward the end of the flow pulse and again about 1 week later, with discrete chlorophyll-*a* data corroborating the time-series data. A peak in chlorophyll at site RVB occurred 3 to 4 weeks after the flow pulse, with total chlorophyll fluorescence values during mid- to late August reaching more than 20 µg L^{-1}. The total chlorophyll fluorescence values measured in the upper Sacramento River at Hood (site SRH, Figure 1) throughout the flow pulse were low, with a mean of 1.41 µg L^{-1} and a max of 2.81 µg L^{-1}.

The Colusa Basin Drain–Ridge Cut and the upper and lower Yolo Bypass regions all showed periods of elevated chlorophyll and DO concentrations above the saturation point before the flow pulse, suggesting high local algal biomass and active growth (Figure 6). These three regions were all observed to have subsequent drops in DO below the saturation point during the peak of the flow pulse. The CSC and lower Sacramento River region sites showed increased DO concentrations above the saturation point, aligning with the two peak chlorophyll events in late July and mid-August as the flow pulse subsided (Figure 6).

The phytoplankton biomass as biovolume (µm^3 mL^{-1}) for all sites primarily comprised diatoms, cryptophytes, and green algae (Table 3, Figure A5 [biovolume], Figure 7 [biomass as µg L^{-1} – C]). The cryptophyte *Plagioselmis* sp. was the most prevalent phytoplankton taxon at

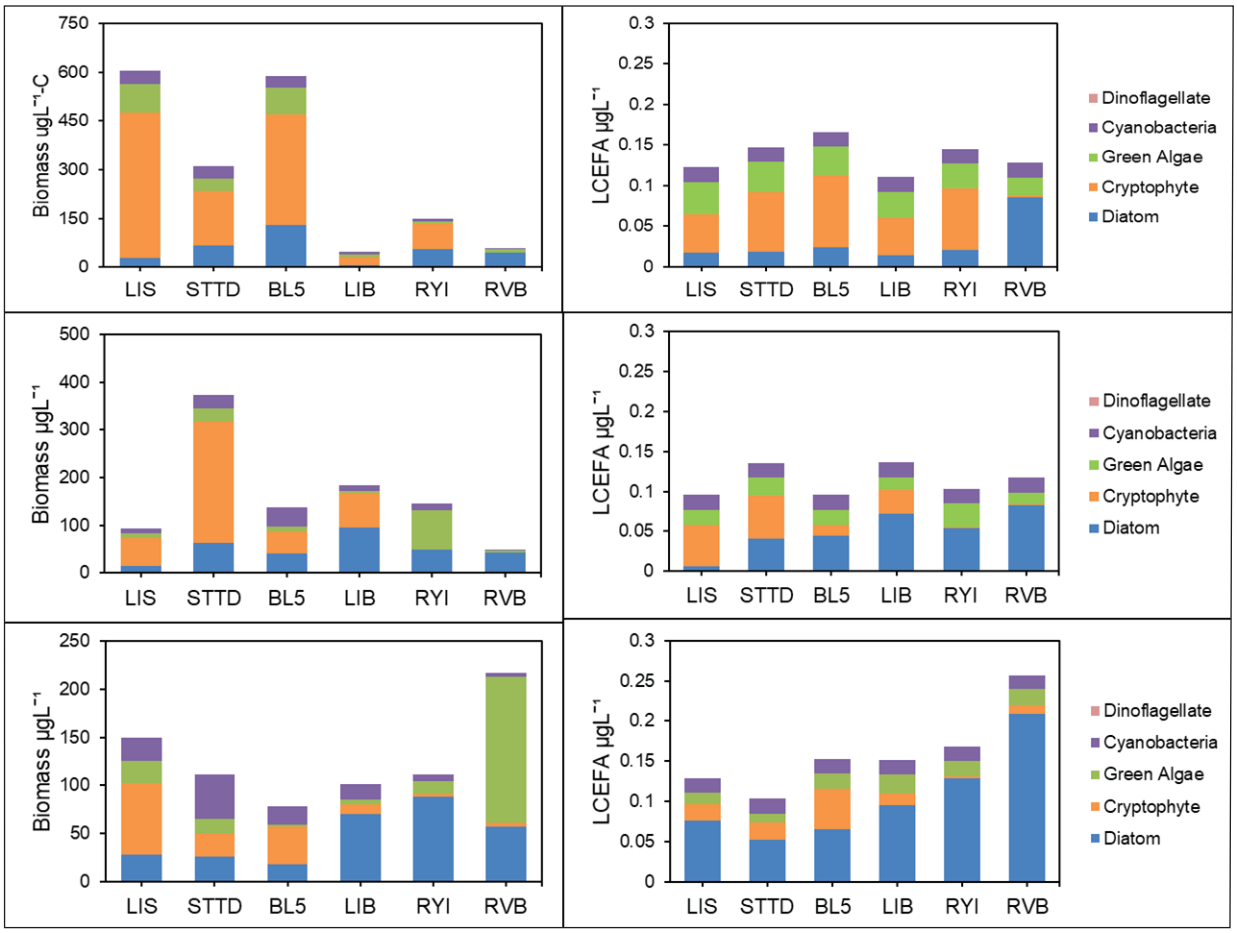

Figure 7 Phytoplankton biomass (µg C L^{-1}) and nutritional indices based on calculated LCEFA % by site across flow action periods, before (**A**), during (**B**), and after (**C**). *Y-axis units for biomass µg L^{-1} vary by flow action periods. From north to south sites include LIS and STTD within the Lower Yolo Bypass; BL5, LIB, and RYI within Cache Slough Complex; RVB at Lower Sacramento River. Phytoplankton biovolume is shown in Appendix Figure A5.

Table 3 Mean biovolume ($\mu m^3\ mL^{-1}$) and percentage of mean total biovolume for phytoplankton taxa compromising ≥ 10% of total biovolume by site. Sites are presented in order from north to south spanning across regions; Lower Yolo Bypass (sites LIS, STTD), Cache Slough Complex (sites BL5, LIB, RYI), and Lower Sacramento River (site RVB).

		Diatoms						Cryptophytes		Green algae				Cyano-bacteria	Total biovolume
		Aulacoseira	*Cyclotella*	*Nitzschia*	*Navicula*	*Ulnaria*	*Bacillaria*	*Plagioselmis*	*Rhodomonas*	*Characium*	*Chlorella*	*Desmodesmus*	*Spirogyra*	*Aphanizomenon*	
Before	LIS	0	1,230,000 (14%)	322,000 (4%)	0	0	0	5,460,000 (63%)	0	0	866,000 (10%)	54,700 (1%)	0	0	8,680,000
	STTD	9,050,000 (71%)	156,000 (1%)	0	0	0	0	1,540,000 (12%)	0	0	405,000 (3%)	0	0	161,000 (1%)	12,800,000
	BL5	21,500,000 (79%)	359,000 (1%)	42,100 (0%)	0	0	0	4,020,000 (15%)	0	0	871,000 (3%)	0	0	0	27,100,000
	LIB	30,000 (3%)	0	96,900 (10%)	0	0	0	459,000 (49%)	84,400 (9%)	0	29,100 (3%)	0	0	0	936,000
	RYI	17,200 (0.2%)	7,440,000 (88%)	24,700 (0%)	0	0	0	855,000 (10%)	0	0	33,400 (0.4%)	0	0	0	8,470,000
	RVB	2,600,000 (87%)	133,000 (4%)	30,100 (1%)	12,500 (0.4%)	0	0	14,700 (0%)	0	0	153,000 (5%)	0	0	0	3,010,000
During	LIS	0	418,000 (7%)	470,000 (8%)	0	0	1,060,000 (17%)	2,530,000 (41%)	912,000 (15 %)	0	114,000 (2%)	135,000 (2%)	0	0	6,210,000
	STTD	2,100,000 (15%)	3,500,000 (24%)	215,000 (1%)	580,000 (4%)	0	0	5,050,000 (35%)	0	0	358,000 (2%)	19,100 (0.1%)	0	0	14,300,000
	BL5	2,460,000 (44%)	681,000 (12%)	61,700 (1%)	0	0	0	1,580,000 (28%)	0	0	82,200 (1%)	0	0	432,000 (8%)	5,570,000
	LIB	10,000,000 (80%)	303,000 (12%)	19,500 (0.2%)	0	0	0	1,420,000 (11%)	0	0	65,000 (1%)	0	0	580,000 (5%)	12,600,000
	RYI	5,890,000 (62%)	124,000 (1%)	88,300 (1%)	0	0	0	8,600 (0.1%)	0	2,650,000 (28%)	89,400 (1%)	274,000 (3%)	0	0	9,570,000
	RVB	1,860,000 (14%)	122,000 (1%)	28,600 (0.2%)	18,600 (0.1%)	308,000 (2%)	0	8,610 (0.1%)	0	0	22,900 (0.2%)	10,800 (0.1%)	11,100,000 (82%)	56,200 (0.4%)	13,600,000
After	LIS	170,000 (5%)	1,050,000 (31%)	126,000 (4%)	854,000 (25%)	97,400 (3%)	0	43,000 (1%)	0	0	76,900 (2%)	456,000 (13%)	0	322,000 (9%)	3,420,000
	STTD	1,560,000 (45%)	404,000 (12%)	201,000 (6%)	182,000 (5%)	58,600 (2%)	0	138,000 (4%)	0	0	39,800 (1%)	0	0	0	3,480,000
	BL5	1,040,000 (59%)	96,500 (5%)	9,200 (1%)	0	11,400 (0.6%)	0	0	0	0	6,780 (0.4%)	14,90 (0.1%)	0	438,000 (25%)	1,770,000
	LIB	1,260,000 (75%)	33,100 (2%)	3,200 (0.2%)	0	186,000 (11%)	0	65,800 (4%)	0	0	28,100 (2%)	0	0	0	1,680,000
	RYI	3,030,000 (75%)	183,000 (5%)	11,800 (0.3%)	35,100 (1%)	99,000 (3%)	0	23,900 (1%)	82,400 (2%)	0	14,100 (0.4%)	2,070 (0.1%)	0	128,000 (3%)	4,020,000
	RVB	3,560,000 (79%)	204,000 (5%)	14,600 (0.3%)	0	597,000 (13%)	0	25,700 (1%)	34,700 (1%)	0	27,300 (0.6%)	2,230 (0.1%)	0	0	4,530,000

the uppermost site LIS in the lower Yolo Bypass region before and during the flow pulse, making up more than 40% of the mean biovolume. The most common taxa observed in samples collected at site STTD and downstream in the CSC and lower Sacramento River regions was the diatom *Aulacoseira* sp., a large-celled filamentous colony-forming taxa (Table 3). Cyanobacteria made up a small amount of the total biovolume in samples collected in all regions, with *Aphanizomenon* sp. being the only taxon that showed up in relatively high biovolumes at site BL5 during and after the flow pulse.

One-way ANOSIM revealed significant differences in mean phytoplankton biovolume ($p < 0.05$,

https://doi.org/10.15447/sfews.2021v19iss3art3

Table 4 Results of ANOSIM and SIMPER analysis based on square-root transformed phytoplankton genera biomass as biovolume (**A**) and zooplankton density (**B**) indicating the strength of separation (ANOSIM R) and the total dissimilarity (% D) between communities and the contribution of the three most discriminating genera to this dissimilarity before, during and after the flow pulse. Significant probabilities (*p*) are in *bold*. Regions are presented in order from north to south; Lower Yolo Bypass (sites LIS, STTD), Cache Slough Complex (sites BL5, LIB, RYI), and Lower Sacramento River (RVB).

	Region	Flow pulse timing analysis	ANOSIM *R*	*p*	% D	SIMPER - Species contribution to the dissimilarity (%)		
A	Lower Yolo Bypass	Before, During	−0.217	0.994	65%	Plagioselmis (22%)	*Aulacoseira* (12%)	Cyclotella (12%)
		Before, after	0.482	**0.002**	68%	Plagioselmis (24%)	*Aulacoseira* (14%)	Chlorella (9%)
		During, After	0.166	**0.049**	71%	Cyclotella (17%)	Plagioselmis (14%)	*Aulacoseira* (12%)
	Cache Slough Complex	Before, During	0.342	**0.003**	71%	*Aulacoseira* (36%)	Plagioselmis (17%)	Cyclotella (14%)
		Before, After	0.583	**0.006**	79%	*Aulacoseira* (27%)	Plagioselmis (20%)	Cyclotella (13%)
		During, After	0.075	**0.001**	62%	*Aulacoseira* (39%)	Plagioselmis (12%)	Cyclotella (9%)
	Lower Sac River	Before, During	−0.111	0.800	66%	*Aulacoseira* (37%)	Spirogyra (25%)	Cyclotella (7%)
		Before, After	−0.333	1.000	59%	*Aulacoseira* (42%)	Cyclotella (11%)	Ulnaria (10%)
		During, After	−0.037	0.457	65%	*Aulacoseira* (36%)	Spirogyra (24%)	Cyclotella (9%)
B	Lower Yolo Bypass	Before, During	0.278	0.143	61%	*Bosmina* (25%)	Rotifers (24%)	Cyclopoid copepodites (12%)
		Before, After	−0.062	0.583	62%	Rotifers (32%)	*Bosmina* (23%)	*Ceriodaphnia* (6%)
		During, After	0.282	**0.038**	51%	Rotifers (24%)	*Bosmina* (14%)	Cyclopoid copepodites (14%)
	Cache Slough Complex	Before, During	0.012	0.342	74%	Rotifers (37%)	*Bosmina* (19%)	Calanoid copepodites (18%)
		Before, After	0.179	0.070	68%	Rotifers (28%)	*Bosmina* (20%)	Calanoid copepodites (20%)
		During, After	0.118	0.127	68%	Rotifers (38%)	Calanoid copepodites (19%)	*Bosmina* (11%)
	Lower Sacramento River	Before, During	1.000	0.333	73%	Rotifers (46%)	*Pseudodiaptomus forbesi* copepodite (18%)	Cyclopoid copepodites (9%)
		Before, After	0.111	0.750	57%	*Pseudodiaptomus forbesi* copepodite (24%)	Calanoid copepodites (18%)	Rotifers (15%)
		During, After	0.500	0.200	74%	Rotifers (58%)	Calanoid copepodites (17%)	

Table 4) before and after the flow pulse in both the lower Yolo Bypass and CSC. The SIMPER analysis on the species contribution to the dissimilarity between mean biovolume in response to the flow pulse showed that more than 70% of dissimilarity before and after the flow pulse could be explained by taxa: *Aulacoseira* sp., *Cyclotella* sp., *Plagioselmis* sp., and *Chlorella* sp. (Table 4; see also Figure A6 for NMDS). There was no significant difference (ANOSIM $p > 0.05$) in the lower Sacramento River when comparing phytoplankton taxa before, during, or after the flow pulse, but this was likely the result of a small sample size. A modeled index was also created for phytoplankton food quality estimates based on mean LCEFA for primary phytoplankton taxonomic groups identified by Galloway and Winder (2015). Food quality as LCEFA increased in all regions after the flow pulse (Figure 7). Both the biomass and food quality of phytoplankton increased in the lower Sacramento region after the flow pulse, with LCEFA concentrations increasing 5-fold (Figure 7C). This food quality index was primarily driven by increases in diatom taxa comprising a higher proportion of the overall regional biomass.

Zooplankton

The zooplankton community varied by region, with the upper freshwater tidal slough habitat in the lower Yolo Bypass (sites LIS, STTD) having higher densities (number m^{-3}) of cladocerans and cyclopoids than the CSC and lower Sacramento River sites (Tables 4 and 5). One-way ANOSIM revealed significant differences only in mean zooplankton densities ($p < 0.05$, Table 4) during and after the flow pulse in the lower Yolo Bypass. The SIMPER analysis on the species contribution to the dissimilarity between mean densities in response to the flow pulse showed that rotifers

Table 5 Mean CPUE (number per cubic meter) and percentage of mean total CPUE of zooplankton taxa compromising ≥ 20% of total CPUE by site. Sites are presented in order from north to south spanning across regions; Lower Yolo Bypass (sites LIS, STTD), Cache Slough Complex (sites BL5, LIB, RYI), and Lower Sacramento River (site RVB).

		Calanoids				Cyclopoids					Cladocerans			
		Pseudo-diaptomus forbesi adult	Calanoid copepodids	*Pseudo-diaptomus forbesi* copepodid	Total CPUE	Cyclopoid copepodids	*Limno-ithona tetraspina*	Eucyclops prion-phorus	Other Cyclopoid adults	Total Cyclopoid CPUE	*Bosmina*	*Cerio-daphnia*	*Diaph-anosoma*	Total Cladocera CPUE
Before	LIS	4,105 (29%)	10,264 (71%)	0	14,370	0	0	0	0	0	107,570 (96%)	0	4,927 (5%)	112,497
	STTD	856 (2%)	34,639 (96%)	0	36,178	2,321 (63%)	1,363 (37%)	0	0	3,684	131,924 (95%)	5,404 (4%)	1,127 (1%)	138,455
	BL5	873 (2%)	40,092 (98%)	0	40,965	748 (100%)	0	0	0	748	46,584 (85%)	4,686 (9%)	3,492 (6%)	55,011
	LIB	642 (9%)	6,448 (91%)	0	7,090	278 (100%)	0	0	0	278	3,906 (82%)	653 (14%)	216 (5%)	4,775
	RYI	0	0	0	24,302	472 (100%)	0	0	0	472	11,597 (96%)	133 (1%)	0	12,102
	RVB	2,197 (8%)	18,316 (65%)	7,766 (28%)	28,280	2,345 (100%)	0	0	0	2,344	1,905 (65%)	733 (25%)	147 (5%)	2,931
During	LIS	250 (20%)	986 (80%)	0	1,236	7,852 (99%)	0	0	41 (1%)	7,893	2,295 (24%)	1,888 (20%)	1,228 (13%)	9,405
	STTD	1,765 (4%)	47,612 (96%)	0	49,377	90,509 (64%)	487 (0.3%)	0	48,496 (35%)	140,569	24,334 (62%)	3,489 (9%)	4,773 (12%)	39,507
	BL5	0	1,425 (93%)	104 (7%)	1,529	52 (100%)	0	0	0	52	676 (55%)	130 (11%)	414 (34%)	1,220
	LIB	0	18,437 (100%)	0	18,438	4,617 (100%)	0	0	0	4,617	8,386 (83%)	1,336 (13%)	267 (3%)	10,108
	RYI	0	21,863 (100%)	0	21,864	1,118 (79%)	298 (21%)	0	0	1,415	9,050 (100%)	0	0	9,050
	RVB	787 (4%)	21,140 (96%)	0	21,927	44 (14%)	284 (87%)	0	0	328	1,401 (100%)	0	0	1,401
After	LIS	243 (1%)	22,172 (93%)	0	23,749	1,947 (89%)	243 (11%)	0	0	2,190	121,533 (97%)	0	3,017 (2%)	126,001
	STTD	244 (2%)	15,346 (98%)	0	15,677	776 (42%)	188 (10%)	0	874 (48%)	1,838	10,490 (82%)	0	1,021 (8%)	12,824
	BL5	27 (1%)	2,875 (99%)	0	2,903	134 (100%)	0	0	0	134	1,960 (81%)	75 (3%)	385 (16%)	2,419
	LIB	286 (3%)	8,191 (97%)	0	8,477	1,492 (57%)	1,119 (43%)	0	0	2,610	1,767 (73%)	95 (4%)	392 (16%)	2,426
	RYI	132 (1%)	11,872 (99%)	0	12,004	597 (35%)	1,117 (65%)	0	0	1,714	1,077 (45%)	1,117 (47%)	170 (7%)	2.403
	RVB	157 (5%)	3,148 (92%)	0	3,388	264 (51%)	0	255 (49%)	0	519	295 (51%)	0	255 (44%)	577

and cladocerans were primarily contributing to differences between flow pulse periods in the lower Yolo Bypass and CSC. Calanoid copepods were more predominant in the CSC and lower Sacramento River regions, contributing more to the dissimilarity before, during, and after the flow pulse. *Bosmina* was the most common cladoceran at all sites, making up ≥95% of the total cladocera in number m^{-3} in the lower Yolo Bypass and ≥65% in the other region sites before the flow pulse. The cyclopoid copepod composition almost entirely comprised copepodite or juvenile life stages throughout the flow pulse. Some noticeable increases during the flow pulse in cladoceran and cyclopoid copepod densities in the CSC at sites LIB and RYI suggests downstream dispersal of upstream sources (Table 5, Figure 8). Both cladocerans and cyclopoid copepod densities at all

https://doi.org/10.15447/sfews.2021v19iss3art3

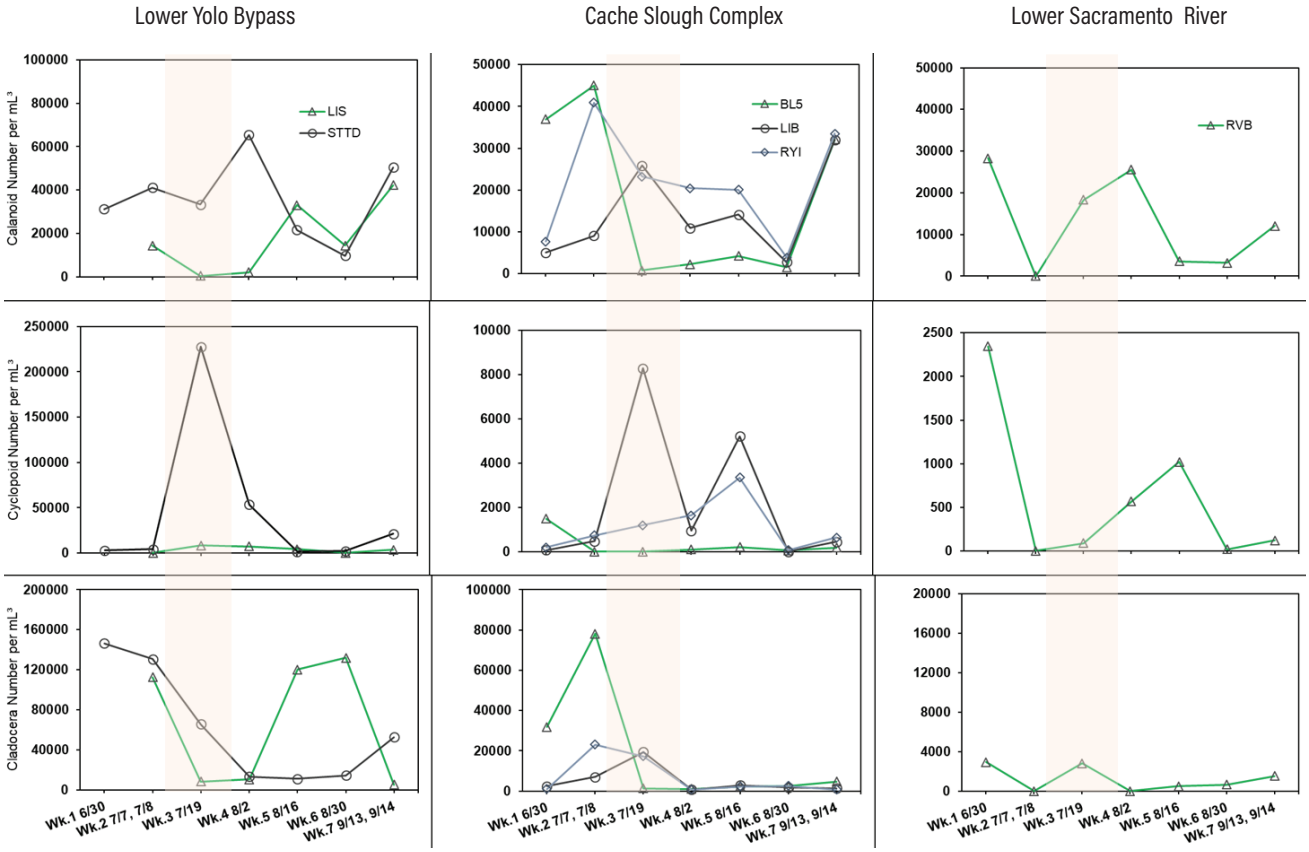

Figure 8 Total CPUE (number per cubic meter) of Calanoid copepods, Cyclopoid copepods, and Cladocerans by region and site across time. The *shaded area* indicates the period of the flow action from July 14–August 1. Sites and regions (north to south) include LIS (*green*) and STTD (*black*) within Lower Yolo Bypass; BL5 (*green*), LIB (*black*), and RYI (*blue*) within Cache Slough Complex; RVB (*green*) at Lower Sacramento River (*black*).

sites showed a significant and positive relationship during the flow pulse (Appendix Table A2). The larger downstream tidal channels in the CSC and lower Sacramento River comprised primarily adult and juvenile calanoid copepods, with *Pseudodiaptomus forbesi* being the most common identified species (see also Appendix Figure A6). The densities of calanoid copepods were relatively high throughout all regions before the flow pulse, and densities in the CSC at site LIB increased 2-fold during the managed flow action (Figure 8). The mechanism of increase was potentially downstream transport from the high upstream densities at sites STTD and BL5 (Table 5, Figure 8). The high densities of juvenile calanoid copepods and low densities of adults in our samples was potentially a product of our near-surface sampling and known vertical migration of copepods during daytime, but it also suggests successful reproduction and recruitment during the study period.

DISCUSSION

Novel Flow Action to Improve Habitat

Freshwater inflow has previously been a major focus of resource management in estuaries, including the San Francisco Estuary, based on the understanding that it supports a broad suite of ecological processes (Jassby et al. 1995; Kimmerer 2002). For example, management of the position of the salinity field (as indexed by the daily-averaged, near-bottom, 2-psu isohaline [X2]) using outflow from the Sacramento–San Joaquin Delta is a major seasonal regulatory criterion in the upper San Francisco Estuary (Sommer 2020; SWRCB 1995)—it is designed as a relatively long-term and geographically broad water quality standard to maintain suitable habitat for a suite of estuarine species. That regulatory framework is not, however, designed to target specific regions, trophic levels, or habitats (e.g., off-channel areas). Given improvements in our understanding of ecological processes in the region, there is a

growing interest in using flow to optimize effects for specific regions or species, particularly in the light of increasing competition for scarce water resources and anticipated alterations to hydrology from climate change. Note, however, that such focused flow actions are not intended as substitutes for broader-scale flow objectives (e.g., low-salinity-zone management in SWRCB 1995); rather, the logic is that there may be ways to improve ecological responses based on the available water. Moreover, such actions can increase our understanding of the effects of flow on habitat and food webs.

Examples of targeted flow actions in the San Francisco Estuary include: (1) managed seasonal inundation experiments in Yolo Bypass to support native fish rearing (Katz et al. 2017; Sommer et al. 2008, 2020b); (2) a summer 2018 effort to direct more low-salinity flow into Suisun Marsh—a key region in the system for many species—using a unique water control structure (Sommer et al. 2020a); and (3) the North Delta flow action described in the current study. However, there is a major conceptual difference between the Suisun Marsh (Sommer et al. 2020a) and Yolo Bypass (Sommer et al. 2008, 2020b) experiments and the current effort. The North Delta flow action represents a rare but increasingly important example of a targeted action in a specific geographic region of the estuary. Specifically, our management action was designed to increase downstream transport of lower trophic level production. In contrast, the Suisun Marsh water control structure and the Yolo Bypass seasonal inundation flow actions were designed to provide fish access to habitat, not to change regional transport patterns.

Below, we elaborate on the major hydrodynamic characteristics of the North Delta flow action, and how this flow experiment affected environmental conditions, with emphasis on lower trophic levels. Overall, the flow action was consistent with our goal to increase downstream transport during a time-period when local water diversions typically heavily affect flows. Hence, this experimental action supported our specific hypothesis that increased net flow in the lower Yolo Bypass (e.g., at LIS) would increase downstream transport of food web organisms and various chemical constituents. The action also provided some support for our second hypothesis that the action could trigger further downstream primary production. However, the second hypothesis will require additional flow actions, monitoring, and modeling to confirm the linkages of increased net flows through the Yolo Bypass and CSC to downstream areas.

Hydrodynamics and Habitat Complexity

The combination of complicated channel and open-water geometry with tidal and anthropogenic forcing from exports and diversions results in complex hydrodynamics and various habitat conditions throughout the study area (Downing et al. 2016; Morgan–King and Schoellhamer 2013; Moyle et al. 2010). For the net flows to be out of the CSC (downstream), the flow through the Toe Drain needs to be larger than the combined diversions, exports, and any evaporation or seepage losses in the CSC. Both the tides and anthropogenic factors strongly influence hydrodynamics in the Yolo Bypass and CSC during periods of low flow (Frantzich et al. 2018). Water export facilities in the CSC include the State Water Project's North Bay Aqueduct, which diverts water from Barker Slough, and numerous agricultural diversions that remove water directly from the Toe Drain and other channels in the CSC. During summer, when freshwater inflow to the CSC is low, the combined effects of these exports, diversions, and net evapotranspiration of water can exceed upstream inflows, and result in a net upstream flow from Cache Slough into the CSC and a net upstream flow in the Toe Drain (Morgan–King and Schoellhamer 2013).

Under normal low-flow conditions, the net northward flow of water through the Toe Drain limits any export of primary and secondary production from this relatively plankton-rich area (Lehman et al. 2010; Owens et al. 2019; Sommer and Mejia 2013) to downstream habitats. Tidal movement of water between the CSC and Cache Slough results in a large exchange of water between the CSC and the larger Delta, but that

https://doi.org/10.15447/sfews.2021v19iss3art3

exchange and supply of primary and secondary production to downstream areas is limited by the net inflow of water to the CSC. With a net upstream flow of Sacramento River water to the CSC from Cache Slough, the water in the lower portion of the CSC is essentially Sacramento River water that arrived via tidal exchange with Cache Slough and the larger Delta (Figure A2A). Since the water exchanged on each tidal cycle has been in the productive CSC for a relatively short period of time, there is little opportunity for additional plankton production from the CSC to be exported to the larger Delta via tidal exchange between the CSC and Cache Slough. Instead, export of plankton production from the CSC occurs to a larger degree during periods of higher flow, when there is a net flow southward out of the CSC.

The flow pulse in 2016 was large enough to overcome the normal upstream net flows (Figure 4) and resulted in a net downstream flow of water and plankton production out of the CSC. This downstream flow of water exports nutrients and plankton from the Toe Drain to the CSC and also increases the net export of water, nutrients, and plankton from the CSC to the larger Delta. By reversing the net flow direction through the study area, the flow pulse had a large effect on the overall hydrodynamics throughout the study area.

Ecological Responses

Regional variability in habitat conditions—including channel geomorphology, connectivity, and hydrology—were key factors underlying physical and chemical differences in the spatial water quality conditions observed before, during, and after the flow pulse. Although, much of the upper connecting channels of the study area are manmade, they likely resemble much of what existed as narrow dendritic channels that once fed into the historical freshwater tidal Delta (Whipple et al. 2012). These historical channels were shallow, often slower-moving, more turbid, and harbor warmer conditions for more optimal primary and secondary productivity. These conditions held true for the Colusa Basin Drain–Ridge Cut Slough and upper Yolo Bypass regions in our study. The added complexity of agricultural structures and drainages in these channels further promotes high residence time, increased specific conductance levels, high DOC, and differing nutrient ratios, allowing us to closely track these source waters as they moved into the downstream channel regions during the flow pulse. The observed downstream increases in primary productivity associated with increased concentrations of DOC and NO_3 + NO_2 suggest added benefits to the ambient conditions for regional plankton communities.

Correlated with differences in habitat conditions, plankton communities within the study regions are also distinct and driven by ambient physical and chemical conditions. As observed in past years, Colusa Basin Drain–Ridge Cut Slough and upper Yolo Bypass regions are known regions of high phytoplankton productivity; these channels maintain low flow and receive ample nutrients to promote high phytoplankton biomass during the summer and fall months (Frantzich et al. 2018). After the flow pulse in 2016, we observed a rapid increase in phytoplankton biomass in the lower Yolo Bypass and CSC regions as high phytoplankton biomass from upstream habitat regions was transported downstream into the lower Yolo Bypass and CSC. The relationships between time-series total chlorophyll fluorescence and DO showed further evidence of associated increased periods of algal photosynthesis. In addition, the lower Sacramento River had increased phytoplankton biomass and improved food quality index a few weeks after positive summer and fall outflow from the Yolo Bypass, a phenomenon similar to that observed in 2011 and 2012 (Frantzich et al. 2018). In prior years, *Aulacoseira* was the primary diatom taxon that made up the observed regional increase in the downstream habitats, because this taxon was exported from the upper study regions. However, the preceding phytoplankton conditions in 2016 were different than in 2011 and 2012, such that a large wide-spread bloom of *Aulacoseira* was already present throughout much of the Delta, and persisted in the CSC and lower Yolo Bypass before the flow pulse. *Aulacoseira*, previously named *Melosira* (Edgar and Theriot 2004), has a unique life history, with known strategies of long-term resting stages within the benthos of

rivers and lakes, and reliance on turbulence from changing wind or inflow to re-suspend and access light for growth (Kilham and Kilham 1975; McQuoid and Hobson 1996). This unique strategy of having a resting stage establishes the ability for *Aulacoseira* to overwinter regionally and repopulate if Delta conditions allow for survival and reseeding. These findings provide evidence of the importance of preceding habitat conditions, and the ability for net positive flows from this action to promote increased primary productivity and the downstream transport of phytoplankton biomass from the CSC and upper channels of the study area.

Corresponding with phytoplankton increases, the flow pulse also demonstrated potential *in situ* production and/or advection of high densities of calanoid copepods, cyclopoid copepods, and cladacerans from upper channels of the Yolo Bypass into the larger tidal channels of the CSC and lower Sacramento River, thereby improving Delta Smelt habitat. The upper channels and floodplain of the Yolo Bypass are known to harbor large densities of cladocerans and cyclopoid copepods (Sommer et al. 2004; Corline et al. 2017; Frantzich et al. 2018); the most prevalent summer and fall zooplankton taxon in the tidal freshwater channels of the CSC and lower Delta is the calanoid copepod *Pseudodiaptomus forbesi* (Kimmerer et al. 2018). Collaborative growth rate studies on *Pseudodiaptomus forbesi* completed in the Yolo Bypass and CSC from 2015 through 2017 demonstrated that high chlorophyll concentrations ($\geq 10\,ug\,L^{-1}$) in these regions resulted in a 50% more measured growth rate than observed in previous studies in other areas of the Delta (Owens et al. 2019). Consistent with our findings, these studies also determined that during periods of net positive outflow in summer and fall (2015 and 2016) the Yolo Bypass acts as a source habitat, exporting zooplankton to downstream regions and improving food availability for Delta Smelt and other native fishes.

Implications and Adaptive Management

The San Francisco Estuary is an exceptionally highly altered ecosystem as a result of urbanization, invasive species, and water delivery and flood infrastructure. However, our study demonstrates that existing water infrastructure can be managed to manipulate summer flows in the North Delta. Consistent with our predictions, the flow pulse quantifiably and meaningfully affected the overall system hydrodynamics and food web, demonstrated by positive summer outflow from the Toe Drain and CSC, improved productivity, and transport of plankton to downstream regions of CSC and the lower Sacramento River. This study provides a good example of the potential value of flow actions to target specific regions or ecological processes (such as food web support) to improve conditions for Delta Smelt and other native fishes. Note that our study was conducted during a single year, which may have had unique characteristics, yet it still provides an example of how a relatively modest change in net flows can generate measurable changes in ecologically relevant metrics. To better understand the underlying mechanisms for flow pulse effects, we recommend actions that may include different timing and magnitudes. Moreover, it would be helpful to address more directly the potential effects on the fish assemblage, including perhaps to answer how Delta Smelt directly respond.

Large-scale adaptive management actions can be particularly challenging in logistical planning and operations, and in predicting how habitat complexity may influence action objectives. The current study showed adaptive management is possible but requires multiple considerations. First, hydrology is important in the adaptive management process; for example, identifying Sacramento River water is available for an experimental action. When stream flows are not available, we found that it may be necessary to consider using alternative water sources, such as agriculture drainage water, which in this area is mainly from rice fields. An additional consideration is that conditions before the flow pulse may influence the outcomes of these adaptive management actions. For example, 2016 was somewhat unusual in that our summer flow action was preceded by a relatively rare Delta-wide phytoplankton bloom, including *Aulacoseira*

https://doi.org/10.15447/sfews.2021v19iss3art3

sp., a diatom. Hence, the presence of *Aulacoseira* may have provided an important "seed stock" that influenced subsequent biological responses. Moreover, large-scale adaptive management to support ecosystems may be more feasible when there is already sufficient infrastructure in place to generate management actions. In the current example, we were able to work with existing water supply, flood, and agricultural infrastructure to implement the flow pulse. Lastly, stake-holder involvement is critical to project success. Our study provides a good example of how involvement from flood and water managers, farmers, and wildlife area managers can lead to novel approaches to improve environmental conditions. Our experience is therefore consistent with other similar projects that included broad stake-holder involvement (Sommer, Schreier et al. 2020).

ACKNOWLEDGEMENTS

The authors acknowledge that this project would not be possible without management support by the Interagency Ecological Program and funding support from California Department of Fish and Wildlife and California Department of Water Resources (CDWR). We would like to thank the CDWR Yolo Bypass Fish Monitoring Program lead field scientist Naoaki Ikemiyagi and all field staff for their many hours of sampling, laboratory work, and data management; Sid Fong and CDWR Bryte Laboratory staff for their water sample analysis and reporting; and BSA Environmental for plankton analysis. We would also like to thank project management support from CDWR personnel Kris Tjernell, Karen Gehrts, and Louise Conrad, as well as managers' review of this manuscript. Lastly, the authors acknowledge the support from local landowners, and managers at GCID, RD108, and CDWR for facilitation of water operations and making this project possible.

REFERENCES

Anchor QEA LLC. 2020. Hydrodynamic modeling of the 2011 through 2019 North Delta food web actions. June 2020. Prepared for California Deparment of Water Resources. 263 p.

[APHA] American Public Health Association. 2012. Standard methods for the examination of water and wastewater. Washington (DC): APHA. 1,496 p.

Bennett WA. 2005. Critical assessment of the Delta Smelt population in the San Francisco Estuary, California. San Franc Estuary Watershed Sci. [accessed 2020 Dec 1];3(2). *https://doi.org/10.15447/sfews.2005v3iss2art1*

Benson BB, Krause D. 1984. The concentration and isotopic fractionation of oxygen dissolved in freshwater and seawater in equilibrium with the atmosphere. Limnol Ocenogr. [accessed 2020 Dec 1];29(3):620-632. *https://doi.org/10.4319/lo.1984.29.3.0620*

Cloern JE, Jassby AD. 2012. Drivers of change in estuarine-coastal ecosystems: discoveries from four decades of study in San Francisco Bay. Rev Geophys. [accessed 2020 Dec 1];50(RG4001):1–33. *https://doi.org/10.1029/2012RG000397*

Corline NJ, Sommer T, Jeffres CA, Katz J. 2017. Zooplankton ecology and trophic resources for rearing native fish on an agricultural floodplain in the Yolo Bypass California, USA. Wetl Ecol. [accessed 2020 Dec 1]; 25(5):533–545. *https://doi.org/10.1007/s11273-017-9534-2*

Deleersnijder E, Campin JM, Delhez EJM. 2001. The concept of age in marine modeling: I. theory and preliminary model results. J Mar Syst. [accessed 2020 Dec 1];28:229–267. *https://doi.org/10.1016/S0924-7963(01)00026-4*

Delhez EJM, Campin JM, Hirst AC, Deleersnijder E. 1999. Toward a general theory of the age in ocean modeling. Ocean Model. [accessed 2020 Dec 1];1:17–27. *https://doi.org/10.1016/S14635003(99)00003-7*

Delta Independent Science Board. 2016. Improving adaptive management in the Sacramento–San Joaquin Delta, Sacramento, CA. [accessed 2020 Jun 25]. 48 p. Available from: *http://deltacouncil.ca.gov/docs/final-delta-isb-adaptive-management-review-report*

Delta Science Program. 2013. Delta science plan. Sacramento (CA): Delta Stewardship Council. [accessed 2020 Jun 25]. Available from: *https://deltacouncil.ca.gov/pdf/delta-plan/2013-delta-plan-combined-chapters.pdf* .

Downing BD, Bergamaschi B, Kendall C, Kraus TEC, Dennis KJ, Von–Dessonneck TS. 2016. Using continuous underway isotope measurements to map water residence time in hydrodynamically complex tidal environments. Environ Sci Technol. [accessed 2020 Dec 1];50(24):13387. *https://doi.org/10.1021/acs.est.6b05745*

Edgar SM, Theriot EC. 2004. Phylogeny of Aulacoseira (*bacillariophyta*) based on molecules and morphology. J Phycol. [accessed 2020 Dec 1];40:772–788. *https://doi.org/10.1111/j.1529-8817.2004.03126.x*

Frantzich J, Sommer T, Schreier B. 2018. Physical and biological responses to flow in a tidal freshwater slough complex. San Franc Estuary Watershed Sci. [accessed 2018 Jun 5];16(1):1–26. *https://doi.org/10.15447/sfews.2018v16iss1/art3*

Galloway AWE, Winder M. 2015. Partitioning the relative importance of phylogeny and environmental conditions on phytoplankton fatty acids. PLoS One. [accessed 2020 Dec 1];10(6). *https://doi.org/10.1371/journal.pone.0130053*

Hammock BG, Hobbs JA, Slater SB, Acuna S, Teh SJ. 2015. Contaminant and food limitation stress in an endangered estuarine fish. Sci Total Environ. [accessed 2020 Dec 1];532:316–326. *https://doi.org/10.1016/j.scitotenv.2015.06.018*

Hennessey TM. 2008. Governance and adaptive management for estuarine ecosystems: the case of Chesapeake Bay. Coastal Manag. [accessed 2020 Dec 1];22(2):119–145. *https://doi.org/10.1080/08920759409362225*

Herbold B, Baltz DM, Brown L, Grossinger R, Kimmerer W, Lehman P, Moyle PB, Nobriga M, Simenstad CA. 2014. The role of tidal marsh restoration in fish management in the San Francisco estuary. San Franc Estuary Watershed Sci. [accessed 2020 Dec 1];12(1). *https://doi.org/10.15447/sfews.2014v12iss1art1*

Jassby AD, Kimmerer WJ, Monismith SG, Armor C, Cloern JE, Powell TM, Schubel JR, Vendlinski TJ. 1995. Isohaline position as a habitat indicator for estuarine populations. Ecol Appl. [accessed 2020 Dec 1];5(1):272–289. *https://doi.org/10.2307/1942069*

Katz JVE, Jefferes C, Conrad JL, Sommer T, Martinez J, Brumbaugh S. 2017. Floodplain farm fields provide novel rearing habitat for Chinook Salmon. PLoS One. [accessed 2020 Dec 1];12(6). *https://doi.org/10.1371/journal.pone.0177409*

Kellar PE, Paulson SA, Paulson LJ. 1980. Methods for biological, chemical, and physical analyses in reservoirs. Lake Mead Limological Research Center Technical Report Series. Vol. 8. Las Vegas (NV): University of Nevada Las Vegas, Department of Biological Sciences. Tech. Report 5. [accessed 2020 Dec 1]. Available from: *https://digitalscholarship.unlv.edu/water_pubs/81*

Kilham SS, Kilham P. 1975. Melosira granulata (ehr.) ralfs: morphology and ecology of cosmopolitan freshwater diatom. Verh Internat Verein Limnol. [accessed 2020 Dec 1];19(4):2716–2721. *https://doi.org/10.1080/03680770.1974.11896368*

Kimmerer WJ. 2002. Physical, biological, and management responses to variable freshwater flow into the San Francisco Estuary. Estuaries. [accessed 2021 Dec 1];25(6B):1275–1290. *https://doi.org/10.1007/BF02692224*

Kimmerer W, Ignoffo TR, Bemowski B, Moderan J, Holmes A, Bergamaschi B. 2018. Zooplankton dynamics in the cache slough complex of the upper San Francisco Estuary. San Franc Estuary Watershed Sci. [accessed 2020 Dec 1];16(3). *https://doi.org/10.15447/sfews.2018v16iss3art4*

Kimmerer W, Lougee L. 2015. Bivalve grazing causes substantial mortality to an estuarine copepod population. J Exp Mar Biol Ecol. [accessed 2020 Dec 1];473:53–63. *https://doi.org/10.1016/j.jembe.2015.08.005*

Kimmerer W, Orsi JJ. 1996. Changes in the zooplankton of the San Francisco Bay Estuary since the introduction of the clam *potamocorbula amurensis*. In: Hollibaugh J, editor. San Francisco Bay: the ecosystem. San Francisco (CA): Pacific Division, American Association for the Advancement of Science. p 403–424.

Kimmerer W, Rose KA. 2018. Individual-based modeling of Delta Smelt population dynamics in the upper San Francisco Estuary. III. Effects of entrainment mortality and changes in prey. Trans Am Fish Soc [accessed 2020 Dec 1];147(1):223–243. *https://doi.org/10.1002/tafs.10015*

Lehman PW, Mayr S, Mecum L, Enright C. 2010. The freshwater tidal wetland Liberty Island, CA was both a source and sink of inorganic and organic material to the San Francisco Estuary. Aquat Ecol. [accessed 2020 Dec 1];44(2):359–372. *https://doi.org/10.1007/s10452-009-9295-y*

Lehman PW, Sommer T, Rivard L. 2008. The influence of floodplain habitat on the quantity and quality of riverine phytoplankton carbon produced during the flood season in San Francisco Estuary. Aquat Ecol. [accessed 2020 Dec 1];42(3):363–378. *https://doi.org/10.1007/s10452-007-9102-6*

Lotze HK. 2010. Historical reconstruction of human-induced changes in U.S. estuaries. In: Gibson RN, Atkinson RJA, Gordon JDM, BarnesH, editors. Oceanography and marine biology: an annual review. Boca Raton (FL): Chapman & Hall. [accessed 2020 Dec 1];48:265–336. *https://doi.org/10.1201/EBK1439821169*

Lotze HK, Lenihan HS, Bourque BJ, Bradbury RH, Cooke RG, Kay MC, Kidwell SM, Kirby MX, Peterson CH, Jackson JBC. 2006. Depletion, degredation, and recovery potential of estuaries and coastal seas. Science. [accessed 2020 Dec 1];312(5781):1806–1809. *https://doi.org/10.1126/science.1128035*

Lucas LV, Thompson JK, Brown LR. 2009. Why are diverse relationships observed between phytoplankton biomass and transport time? Limnol Oceanogr. [accessed 2020 Dec 1];54(1):381–390. *https://doi.org/10.4319/lo.2009.54.1.0381*

MacWilliams ML, Bever AJ, Gross ES, Ketefian GS, Kimmerer W. 2015. Three-dimensional modeling of hydrodynamics and salinity in the San Francisco Estuary: an evaluation of model accuracy, X2, and the low salinity zone. San Franc Estuary Watershed Sci. [accessed 2020 Dec 1];13(1). *https://doi.org/10.15447/sfews.2015v13iss1art2*

MacWilliams ML, Gross ES. 2007. Untrim San Francisco Bay-Delta model calibration report. Delta Risk Management Study. Prepared for the California Department of Water Resources. 101 p.

Mahardja B, Hobbs JA, Ikemiyagi N, Benjamin A, Finger AJ. 2019. Role of freshwater floodplain–tidal slough complex in the persistence of the endangered Delta Smelt. PLOS ONE. [accessed 2020 Dec 1];14(1). *https://doi.org/10.1371/journal.pone.0208084*

McQuoid MR, Hobson LA. 1996. Diatom resting stages. J Phycology. [accessed 2020 Dec 1];32:889–902. *https://doi.org/10.1111/j.0022-3646.1996.00889.x*

Menden–Deuer S, Lessard EJ. 2000. Carbon to volume relationships for dinoflagellates, diatoms, and other protist plankton. Limnol Ocenogr. [accessed 2020 Dec 1];45(3):569–579. *https://doi.org/10.4319/lo.2000.45.3.0569*

Minitab 16 Statistical Software. 2010. [computer software]. [accessed 2020 Dec 1]. State College (PA): Minitab, Inc. Available from: *https://www.minitab.com*

Morgan–King TL, Schoellhamer DH. 2013. Suspended-sediment flux and retention in a backwater tidal slough complex near the landward boundary of an estuary. Estuaries Coasts. [acessed 2020 Dec 1];36(2):300–318. *https://doi.org/10.1007/s12237-012-9574-z*

Moyle PB, Hobbs JA, Durand JR. 2018. Delta Smelt and water politics in California. Fisheries. [acessed 2020 Dec 1];43(1). *https://doi.org/10.1002/fsh.10014|*

Moyle PB, Lund JR, Bennett WA, Fleenor WE. 2010. Habitat variability and complexity in the upper San Francisco Estuary. San Franc Estuary Watershed Sci. [accessed 2020 Dec 1];8(3). *https://doi.org/10.15447/sfews.2010v8iss3art1*

Nichols FH, Cloern JE, Luoma SN, Peterson DH. 1986. The modification of an estuary. Science. [accessed 2020 Dec 1]231:567–573. *https://doi.org/10.1126/science.231.4738.567*

[NMFS] National Marine Fisheries Service. 2009. Biological opinion and conference opinion on the long-term operations of the Central Valley Project and State Water Project. NMFS Consultation Number: SWR-2008/09022. Long Beach (CA): Southwest Region. [accessed 2020 Dec 1]. Available from: *https://www.fisheries.noaa.gov/resource/document/biological-opinion-and-conference-opinion-long-term-operations-central-valley*

Owens S, Ignoffo TR, Frantzich J, Slaughter A, Kimmerer W. 2019. High growth rates of dominant calanoid copepod in the northern San Francisco Estuary. J Plankton Res [accessed 2020 Apr 14]; 41(6):939–954. *https://doi.org/10.1093/plankt/fbz064*

Rose KA, Kimmerer WJ, Edwards KP, Bennett WA. 2013. Individual-based modeling of Delta Smelt population dynamics in the upper San Francisco Estuary: II. alternative baselines and good versus bad years. Trans Am Fish Soc [accessed 2020 Dec 1];142(5):1260–1272. *https://doi.org/10.1080/00028487.2013.799519*

Service RF. 2007. Delta blues, California style. Science. [accessed 2020 Dec 1];317(5837):442–445. *https://doi.org/10.1126/science.317.5837.442*

Sommer T. 2020. How to respond? An introduction to current Bay–Delta natural resources management options. San Franc Estuary Watershed Sci. [accessed 2020 Dec 1];18(3). *https://doi.org/10.15447//sfews.2020v18iss3art1*

Sommer T, Harrell B, Nobriga M, Brown R, Moyle P, Kimmerer W, Schemel L. 2001. California's Yolo Bypass: evidence that flood control can be compatible with fisheries, wetlands, wildlife, and agriculture. Fisheries [accessed 2020 Dec 1];26(8):6–16. *https://doi.org/10.1577/1548-8446(2001)026<0006:cyb>2.0.co;2*

Sommer T, Harrell WC, Matica Z, Feyrer F. 2008. Habitat associations and behavior of adult and juvenile splittail (cyprinidae: *Pognichthys macrolepidotus*) in a managed seasonal floodplain wetland. San Franc Estuary Watershed Sci. [accessed 2020 Dec 1];6(2). *https://doi.org/10.15447/sfews.2008v6iss2art3*

Sommer T, Hartman R, Koller M, Koohafkan M, Conrad JL. 2020a. Evaluation of a large-scale flow manipulation to the upper San Francisco Estuary: response of habitat conditions for an endangered native fish. PLoS One. [accessed 2020 Dec 1];15(10). *https://doi.org/10.1371/journal.pone.0234673*

Sommer T, Mejia F. 2013. A place to call home: a synthesis of Delta Smelt habitat in the upper San Francisco Estuary. San Franc Estuary Watershed Sci. [accessed 2020 Dec 1];11(2). *https://doi.org/10.15447/sfews.2013v11iss2art4*

Sommer T, Schreier B, Conrad JL, Takata L, Serup B, Titus R. 2020b. Farm to fish: lessons from a multi-year study on agricultural floodplain habitat. San Franc Estuary Watershed Sci. [accessed 2020 Dec 1];18(3). *https://doi.org/10.15447/sfews.2020v18iss3art4*

Sommer TR, Armor C, Baxter RD, Breuer R, Brown LR, Chotkowski M, Culberson S, Feyrer F, Gingras M, Herbold B, et al. 2007. The collapse of pelagic fishes in the upper San Francisco Estuary: El Colapso de los Peces Pelagicos en La Cabecera Del Estuario San Francisco. Fisheries. [accessed 2020 Dec 1]; 32(6):270–277. *https://doi.org/10.1577/1548-8446(2007)32[270:TCOPFI]2.0.CO;2*

Sommer TR, Harrell WC, Solger AM, Tom B, Kimmerer W. 2004. Effects of flow variation on channel and floodplain biota and habitats of the Sacramento River, California, USA. Aquatic Conservation–Marine and Freshwater Ecosystems. [accessed 2020 Dec 1];14(3):247–261. *https://doi.org/10.1002/aqc.620*

[SWRCB] State Water Resources Control Board. 1995. Water quality control plan for the San Francisco Bay/Sacramento–San Joaquin Delta estuary. Sacramento (CA): SWRCB/CEPA. [accessed 2020 Dec 1]. 55 p. Available from: *https://www.waterboards.ca.gov/waterrights/water_issues/programs/bay_delta/wq_control_plans/1995wqcp/docs/1995wqcpb.pdf*

Thom RM. 2000. Adaptive management of coastal ecosystem restoration projects. Ecol Eng [accessed 2020 Dec 1];15(1):365–372. *https://doi.org/10.1016/S0925-8574(00)00086-0*

Thomson JR, Kimmerer WJ, Brown LR, Newman KB, Mac Nally R, Bennett WA, Feyrer F, Fleishman E. 2010. Bayesian change point analysis of abundance trends for pelagic fishes in the upper San Francisco Estuary. Ecol Appl [accessed 2020 Dec 1];20(5):1431–1448. *https://doi.org/10.1890/09-0998.1*

[IOOS] Integrated Ocean Observing System. 2020. Manual for real-time quality control of in situ temperature and salinity data version 2.1: a guide to quality control and quality assurance of in situ temperature and salinity observations. Washington, D.C.: National Oceanic and Atmospheric Administration. [accessed 2020 Dec 1]. p. 1–55. *https://doi.org/10.25923/x02m-m555*

Utermöhl H. 1958. Zur vervollkommnung der quantitativen phytoplankton-methodik. [Methods of collecting plankton for various purposes are discussed.] Verh Internat Verein Theor Angew Limnol. [accessed 2020 Dec 1];9:1–38. *https://doi.org/10.1080/05384680.1958.11904091*

Primer e. v7. c2017. In: Clarke KRaRNG, editor. User Manual/Tutorial. Plymouth: PRIMER-E. Available from: *https://www.primer-e.com/*

Wagner RJ, Boulger Jr RW, Oblinger CJ, Smith BA. 2006. Guidelines and standard procedures for continuous water-quality monitors: station operation, record computation, and data reporting. Techniques and Methods Report 1-D3. USGS Publications Warehouse. [accessed 2020 Dec 1]. *https://doi.org/10.3133/tm1D3*

Wang R, Ateljevich E. 2012. Methodology for flow and salinity estimates in the Sacramento–San Joaquin delta and Suisun Marsh, 23rd annual progress report to the State Water Resources Control Board. California Department of Water Resources, Bay–Delta Office, Delta Modeling Section. [accessed 2020 Dec 1]. Available from: *https://www.waterboards.ca.gov/waterrights/water_issues/programs/bay_delta/california_waterfix/docs/20160712_deirdre_refer_report.pdf*

Whipple AA, Grossinger RM, Rankin D, Standford B, Askevold RA. 2012. Sacramento–San Joaquin Delta historical ecology investigation: exploring pattern and process. Prepared for the California Department of Fish and Game and Ecosystem Restoration Program. SFEI Contribution No. 672. Richmond (CA): San Francisco Estuary Institute–Aquatic Science Center. [accessed 2020 Dec 1]. Available from: *https://www.sfei.org/documents/sacramento-san-joaquin-delta-historical-ecology-investigation-exploring-pattern-and-proces*

Winder M, Jassby AD. 2011. Shifts in zooplankton community structure: Implications for food web processes in the upper San Francisco Estuary. Estuaries Coasts. [accessed 2020 Dec 1];34(4):675–690. *https://doi.org/10.1007/s12237-010-9342-x*

Worm B, Barbier EB, Beaumont N, Emmett Duffy J, Folke C, Halpern BS, Jackson JBC, Lotze HK, Micheli F, Palumbi SR, et al. 2006. Impacts of biodiversity loss on ocean ecosystem services. Science [accessed 2020 Dec 1];314(5800):787–790. *https://doi.org/10.1126/science.1132294*

Zedler JB. 2016. Integrating traditional ecological knowledge with adaptive restoration. Ecosyst Health Sustain. [accessed 2020 Dec 1];2(6):1–3. *https://doi.org/10.1002/ehs2.1222*